



HAL
open science

Industrial symbiosis of anaerobic digestion and pyrolysis: Performances and agricultural interest of coupling biochar and liquid digestate

Saida Tayibi, Florian Monlau, Frederic Marias, Nicolas Thevenin, Raquel Jimenez, Abdallah Oukarroum, Adil Alboukhas, Youssef Zeroual, Abdellatif Barakat

► To cite this version:

Saida Tayibi, Florian Monlau, Frederic Marias, Nicolas Thevenin, Raquel Jimenez, et al.. Industrial symbiosis of anaerobic digestion and pyrolysis: Performances and agricultural interest of coupling biochar and liquid digestate. *Science of the Total Environment*, 2021, 793, pp.148461. 10.1016/j.scitotenv.2021.148461 . hal-03280487

HAL Id: hal-03280487

<https://hal.inrae.fr/hal-03280487>

Submitted on 2 Aug 2023

HAL is a multi-disciplinary open access archive for the deposit and dissemination of scientific research documents, whether they are published or not. The documents may come from teaching and research institutions in France or abroad, or from public or private research centers.

L'archive ouverte pluridisciplinaire **HAL**, est destinée au dépôt et à la diffusion de documents scientifiques de niveau recherche, publiés ou non, émanant des établissements d'enseignement et de recherche français ou étrangers, des laboratoires publics ou privés.



Distributed under a Creative Commons Attribution - NonCommercial | 4.0 International License

1 **Industrial symbiosis of anaerobic digestion and pyrolysis: performances and**
2 **agricultural interest of coupling biochar and liquid digestate**

3
4 Saida Tayibi^{1, 2, 3, 4}, Florian Monlau^{3*}, Frederic Marias⁵, Nicolas Thevenin⁶, Raquel
5 Jimenez³, Abdallah Oukarroum², Adil Alboukhas^{1,7}, Youssef Zeroual⁸, and Abdellatif
6 Barakat^{1,2*}

7 ¹IATE, University of Montpellier, INRAE, Agro Institut of Montpellier, Montpellier, France

8 ²Mohammed VI Polytechnic University (UM6P), Ben Guerir, Morocco

9 ³APESA, Pôle Valorisation, Cap Ecologia, Lescar, France

10 ⁴LIMAT, Faculté des Sciences Ben M'Sik, Université Hassan II de Casablanca, Morocco

11 ⁵Laboratoire de Thermique Energétique et Procédés – IPRA, EA1932, Université de Pau et des Pays
12 de l'Adour/E2S, UPPA, 64000 Pau, France

13 ⁶RITTMO Agroenvironnement-ZA Biopôle – 37 rue de Herrlisheim– CS 800 23 – 68025 COLMAR
14 CEDEX, France

15 ⁷Laboratoire des procédés chimiques et matériaux appliqués (LPCMA), Faculté polydisciplinaire de
16 Béni-Mellal, Université Sultan Moulay Slimane, BP 592, 23000 Béni-Mellal, Morocco

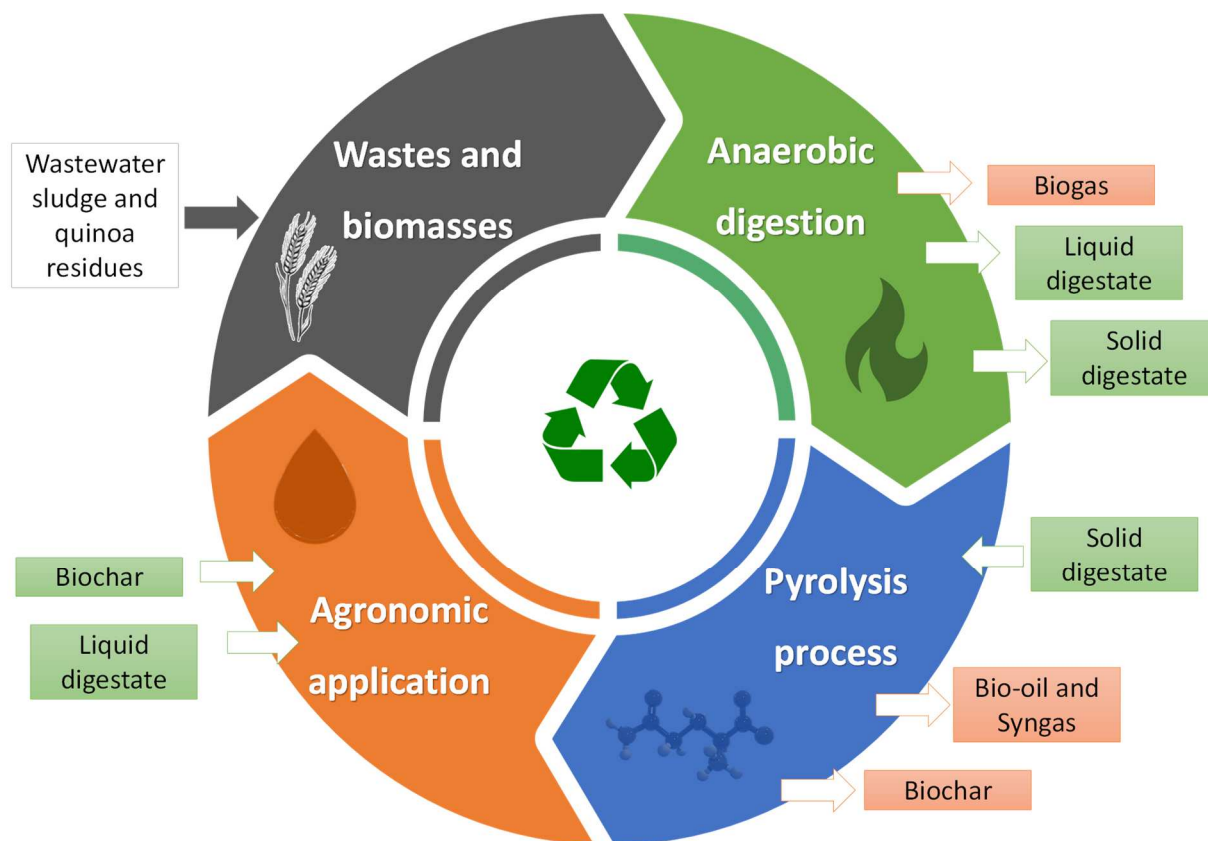
17 ⁸Situation Innovation, OCP Group, Complexe industriel Jorf Lasfar, El Jadida, Morocco

18

19 *Corresponding author: Florian Monlau; Email: florian.monlau@apesa.fr;
20 abdellatif.barakat@inrae.fr Tel: +33688491845

21

22 **GRAPHICAL ABSTRACT**



23

24

25 **Keywords:** Anaerobic digestion, biochar, biogas, bio-oil, mineralization, plant growth tests,
26 syngas

27

28 **Abbreviations:**

29 **AD:** Anaerobic digestion

30 **B25:** Biochar at 25 tons/ha

31 **B50:** Biochar at 50 tons/ha

32 **BMP:** Biochemical Methane Potential

33 **CHP:** Cogeneration Heat and Power

34 **COD:** Chemical Oxygen Demand

35 **CSTR:** Continuous Stirred Tank Reactor

36 **DM:** Dry Matter

37 **EBC:** European Biochar Certificate

38 **IBI:** International Biochar Initiative

39 **IF:** Industrial Fertilizer (DAP and ammonium nitrate)

40 **LD:** Liquid Digestate

41 **VS:** Volatile Solid

42

43 **ABSTRACT**

44 The sustainability of the anaerobic digestion industry is closely related to proper digestate
45 disposal. In this study, an innovative cascading biorefinery concept coupling anaerobic
46 digestion and subsequent pyrolysis of the digestate was investigated with the aim of
47 enhancing the energy recovery and improving the fertilizers from organic wastes. Continuous
48 anaerobic co-digestion of quinoa residues with wastewater sludge (45/55% VS) exhibited
49 good stability and a methane production of 219 NL CH₄/ kg VS. Subsequent pyrolysis of the
50 solid digestate was carried out (at 500 °C, 1 h, and 10 °C/min), resulting in a products
51 distribution of 40 wt% biochar, 36 wt% bio-oil, and 24 wt% syngas. The organic phase (OP)
52 of bio-oil and syngas exhibited higher and lower heating values of 34 MJ/kg and 11.8
53 MJ/Nm³, respectively. The potential synergy of coupling biochar with liquid digestate (LD)

54 for agronomic purposes was investigated. Interestingly, coupling LD (at 170 kgN/ha) with
55 biochar (at 25 tons/ha) improved the growth of tomato plants up to 25% compared to LD
56 application alone. In parallel, co-application of biochar with LD significantly increased the
57 ammonia volatilization (by 64%) compared to LD application alone, although their
58 simultaneous use did not impact the C and N mineralization rates.

59 **1. Introduction**

60 The increase in the world's population is creating environmental issues such as over-
61 exploitation of fossil fuels and the accumulation of wastes. In recent decades, the scientific
62 community has increasingly engaged in the development of processes that optimize the
63 recovery and use of organic wastes (biowastes, agricultural wastes, agro-industrial wastes,
64 urban wastes, etc.) in a diverse range of products according to the concept of environmental
65 biorefineries (Demichelis et al., 2020; Monlau et al., 2015a). Morocco has rapidly
66 transformed into a largely urban society over the past decade, with approximately 60% of its
67 citizens now living in cities and urban areas due to a trend of rural migration to coastal
68 centers. The high population growth rate in urban agglomerations in recent years has been
69 accompanied by environmental problems such as an increase in wastes and effluents
70 (Alhamed et al., 2018; Belloulid et al., 2017). Morocco has achieved significant improvement
71 in the wastewater sector in the past ten years, and 123 wastewater treatment plants (WWTP)
72 have been built, increasing the treatment capacity to 900 million m³ per year (Alhamed et al.,
73 2018). In 2015, the potential production of sludge in Morocco at the level of WWTP was
74 estimated to 155,450 tons of dry matter (Belloulid et al., 2017).

75 Anaerobic digestion (AD) is a well-known process that has been used for many decades to
76 treat organic wastes, such as wastewater sludges (Sawatdeenarunat et al., 2016). This process
77 transforms organic matter in the absence of oxygen into biogas (a mixture of CH₄ and CO₂)
78 and an undegraded residue called digestate (Monlau et al., 2015b). Biogas is a source of

79 energy that is generally used to generate heat and electricity through cogeneration and a heat
80 power system or it can be injected into the natural gas grid after an upgrading process
81 (Roubaud and Favrat, 2005). Nonetheless, mono-AD of organic wastes is limited by the need
82 to maintain an optimal C/N ratio between 15 and 30 (Chandra et al., 2012), which can lead to
83 instability and decreased performance (Sawatdeenarunat et al., 2016). Anaerobic co-digestion
84 with lignocellulosic biomass is a promising technology to improve digester performance with
85 wastewater sludge by improving the C/N ratio (Giuliano et al., 2013; Zhao et al., 2018).
86 Despite the potential of co-digestion technology, lignocellulosic biomass as a co-substrate can
87 lead to a significant increase in the volume of digestate, thus requiring a final
88 elimination/valorization step (González et al., 2020). Generally, the anaerobic digestate is
89 separated into a liquid fraction (rich in nutrients, especially N and K) and a solid fraction rich
90 in P and fibers that are mostly separated by a filter press, centrifuge, or a vibrating sieve
91 (Akhiar et al., 2017).

92 The cascading biomass valorization approach by coupling two or three processes has become
93 a new strategy to achieve the “zero waste” goal at the industrial scale. Recently, the coupling
94 of anaerobic digestion (AD) and pyrolysis processes through the pyrolysis of solid digestate
95 has been considered as a solution to the challenge of AD digestate management and a way to
96 increase the sustainability of the entire process by the production of a higher amount of
97 biofuels (syngas and bio-oil) (Fabbri and Torri, 2016; Ghysels et al., 2020; González et al.,
98 2020; Pecchi and Baratieri, 2019). Pyrolysis is a thermochemical process in which biomass is
99 thermally degraded under an inert or a very low stoichiometric oxygen atmosphere (Tripathi
100 et al., 2016), yielding three products: syngas (mainly CO₂, H₂, and CO), bio-oil (composed of
101 an organic and an aqueous phases), and biochar (Monlau et al., 2015). Syngas can be
102 converted into heat or heat/electricity (combined heat and power, CHP) alone or mixed with
103 biogas in boilers and engines (Seyedi et al., 2019). The organic phase of bio-oil can be used as

104 a fuel, or it can be added to petroleum refinery products or upgraded by catalysts to produce
105 premium-grade refined fuels, or it may have use as building blocks (Pütün et al., 2005)
106 whereas the aqueous phase can be recirculated as feedstock for the AD process (Torri and
107 Fabbri, 2014). The energetic interest of coupling AD and pyrolysis compared to stand-alone
108 AD has been demonstrated previously (Ghysels et al., 2020; Monlau et al., 2015b). In parallel,
109 González-Arias et al. (2019) demonstrated that the combined approach of pyrolysis and
110 digestion solves the digestate disposal problem by generating biochar. Indeed, biochar, which
111 is the carbonaceous material obtained from pyrolysis, has several advantages (stable C,
112 hygienization, water retention, etc.) and it can be used in several environmental applications
113 (Abdeljaoued et al., 2020). For instance, biochar has gained much attention in recent decades
114 due to its potential to enhance soil quality and soil preservation, as well as mitigation of
115 climate change by carbon sequestration (Fernández et al., 2014; Semida et al., 2019).

116 Nonetheless, although coupling AD and pyrolysis has been well described and discussed in
117 the literature from an energetic point of view, less information is available regarding the use
118 of biochar derived from solid digestate for agronomic applications used alone or in
119 combination with liquid digestate (Glaser et al., 2015; Opatokun et al., 2017; Tayibi et al.,
120 2021). Ronga et al. (2020) assessed the effect of combining biochar (from pine wood chips)
121 with LD (from AD of a mixture of maize silage, triticale silage, cow slurry, and grape stalks)
122 on the fruit yield of tomatoes produced by organic farming. The results demonstrated that
123 tomato plants fertilized with LD and biochar achieved a maximum yield of 72 tons/ha, while
124 the lowest production of 47 tons/ha was recorded with unfertilized plants (Ronga et al., 2020).
125 Similarly, Tayibi et al., (2020a) investigated the coupling of LD with biochar (produced from
126 the solid digestate fraction) for agronomic applications on nutrient leaching and wheat
127 growth. Interestingly, the addition of biochar increased the cumulative leaching of all
128 nutrients, except nitrate, with a significant decrease of 82% at 50 tons/ha, compared to soil

129 treated only with LD alone. In parallel, co-application of biochar and LD improved the aerial
130 dry biomass production of wheat (up to 27.5%) compared to soil treated only with LD.
131 Nonetheless, there is still little information available regarding the coupling of LD and
132 biochar, not only in terms of crop yields but also on changes in the physicochemical
133 properties of soil. The present study, therefore, evaluated the following:

- 134 • The performance of a continuous stirred reactor (CSTR) at a pilot scale for co-
135 digestion of quinoa residues and wastewater sludge;
- 136 • The pyrolysis products (biochar, bio-oil, and syngas) from a solid digestate at 500 °C,
137 1 h, and 10 °C/min;
- 138 • Characterization of the syngas, bio-oil, and biochar by evaluation of the content of the
139 inorganic elements contained in the biochar with the range suggested by the
140 International Biochar Initiative (IBI) and the European Biochar Certificate (EBC).
- 141 • The phytotoxicity (germination index) of co-application of biochar (25 tons/ha and 50
142 tons/ha) and LD (170 kg N /ha) on tomato plants;
- 143 • The effect of co-application of biochar (25 tons/ha) and liquid digestate (170 kg N/ha)
144 on microbial respiration (CO₂), the mineralization of nitrogen, and the volatilization of
145 ammonia.

146 **2. Materials and Methods**

147

148 **2.1. Feedstocks, inoculum, and soil properties**

149 Two different residues were used for the anaerobic digestion tests: wastewater sludge and
150 quinoa residues. The wastewater sludge was collected from a WWTP located in Lescar
151 (France) and stored at -16 °C. Quinoa residues were collected from a private farm located in
152 Benguerir (Morocco), the residues were dried at 40 °C for three days and crushed twice using
153 an electric vegetable mill (Ge250, Stihl Viking®, Germany). The inoculum used for the
154 biochemical methane potential (BMP) tests and for the semi-continuous assays was an

155 internal mesophilic inoculum produced at the APESA center and fed with a mixture of
156 wastewater sludge and grass. For the agronomic tests, an agricultural soil sampled at the
157 surface (0-25 cm) was collected at the INRAE site in Mauguio (15.8 km from Montpellier,
158 France). The soil was air-dried and passed through a 2-mm sieve to remove large fragments.
159 The main characteristics of the soil were (per thousand parts of raw material): 210 parts clay
160 ($< 2\mu\text{m}$), 93 parts fine silt (2 to 20 μm), 208 parts coarse silt (20 to 50 μm), 196 parts fine
161 sand (50 to 200 μm), and 302 parts coarse sands (200 to 2,000 μm). The soil was classified as
162 a clay loamy soil. Some of the other characteristics of the soil were a pH of 7.4 ± 0.1 (water),
163 $1.9 \pm 0.2\%$ organic matter, a C/N ratio of 10.1, a total nitrogen (TN) content of 0.1 wt%,
164 0.1 ± 0.02 g/kg phosphorus (P_2O_5), 0.4 g/kg potassium (K_2O), and a 9.9 ± 1.0 cmol (+)/kg
165 cation exchange capacity (CEC). Two commercial fertilizers were used: DAP ($(\text{NH}_4)_2\text{HPO}_4$,
166 characterized by 18 wt% N- NH_4 and 46 wt% P- P_2O_5 , provided by the Cherifian Office for
167 Phosphates (OCP) company and complemented with ammonium nitrate (NH_4NO_3) (99%),
168 from Sigma-Aldrich[®], to obtain a ratio of 170 kg N/ha.

169 **2.2. Anaerobic digestion (AD) process**

170

171 The BMP tests were performed under anaerobic mesophilic conditions (35 ± 2 °C, pH = 7)
172 and in duplicate with a working volume of 500 mL at a substrate inoculum (S/I) ratio of 0.35
173 according the recommendations made in the European Interlaboratory study (Hafner et al.,
174 2020). A blank control (only the inoculum) was carried out in parallel with the other
175 biomasses that were tested (wastewater sludge and quinoa residues) to subtract the amount of
176 biogas generated by just the inoculum. Once the bottle was prepared, it was purged with
177 nitrogen gas (N_2) to maintain anaerobic conditions. The bottles were then sealed and placed in
178 an oven at 35 ± 2 °C to maintain mesophilic conditions. The biogas production was monitored
179 daily by pressure measurements using a manometer with an LC display (Testo 502,
180 TESTOON, France). The composition of the biogas (H_2 , O_2 , N_2 , CH_4 , CO_2 , and H_2S) was

181 determined using a micro gas chromatograph (490, Agilent Technology, USA). The first
182 column (Molsieve 5Å PLOT) was used at 110 °C to separate the O₂, N₂, and CH₄, and the
183 second column (HayeSep A) was used at 70 °C to separate the CO₂ from the other gases. The
184 injector and the detector temperatures were 110 °C and 55 °C, respectively. Detection of the
185 gaseous compounds was performed using a thermal conductivity detector. The calibration was
186 performed with two standard gases composed of either 9.5% CO₂, 0.5% O₂, 81% N₂, and 10%
187 CH₄ or 35% CO₂, 5% O₂, 20% N₂, and 40% CH₄ (Air Liquide®). All of the results are
188 presented under standardized conditions of temperature and pressure (P_{atm}, 0 °C). After
189 determination of the BMP of the substrates (quinoa residues and wastewater sludge), a
190 continuously stirred tank reactor (CSTR) assay was set up with a total working volume of 20
191 L under mesophilic conditions (35 ± 2 °C) and homogeneity was maintained using a
192 continuous agitation system. The reactor was initially supplied with mesophilic inoculum as
193 previously described. The feedstock input and the discharge digestate were performed
194 manually once a day (5 days per week). The feedstock mixture was composed of 42.5% VS
195 wastewater sludge and 57.5% VS quinoa residues. The organic load rate and the hydraulic
196 retention time were set at 2.06 g VS/m³ day and 41 days, respectively. The CSTR was
197 monitored by measurement of the pH and the temperature on a daily basis, the FOS/TAC
198 (Free Organic Acids / Total Inorganic Carbonate) ratio twice a week, and the volatile fatty
199 acids (VFAs) as well as the ammonium concentration once a week. Details for all the
200 experimental protocols are provided in the previous section. Measurement of the Dry Matter
201 (DM) and the Volatile Solid (VS) contents of the digestate was carried out every weekend.
202 The biogas produced was recorded every day by a PC system connected to a Ritter volumetric
203 counter cell. The biogas was collected in a gas pocket directly connected to the gas meter; the
204 analysis of the biogas was carried out 5 days/week using micro gas chromatography (490,
205 Agilent Technology, USA) as previously described. At the end of the process, a solid-liquid

206 separation was carried out using a wine press. A mass balance of the chemical oxygen
207 demand (COD) was also carried out at the end of the process. To assess the mass balance, it
208 was assumed that 350 NL CH₄ can be produced per kg of COD. The COD of the solid
209 digestate was assessed by a modified protocol using a double acid hydrolysis of biomasses as
210 described by Cazaudehore et al. (2019). The supernatant liquids from the solid fraction and
211 the LD were analyzed for COD using commercial kits (Spectroquant 14,155, Merck,
212 Germany). The concentrations ranged from 500 to 10,000 mg COD/L. The tubes were then
213 heated to 148 °C in a preheated thermoreactor for 120 min. Finally, the COD was measured
214 by an automatic spectrophotometer (photoLab[®] S6, WTW, Germany).

215 **2.3 Pyrolysis test of the solid digestate**

216 The dried solid digestate sample (approximately 300 g) was subjected to pyrolysis in a steel
217 reactor. Before the pyrolysis, the basket of feedstock and the furnace were purged with N₂ for
218 30 min to ensure an oxygen-free environment. The experiments were then carried out in
219 duplicate at 500 °C with a heating rate of 10 °C/min, for 1 hour at high temperature. The
220 collected pyrolysis products were biochar, bio-oil (condensable gas), and syngas (non-
221 condensable gas). The furnace was then cooled to 25 °C under nitrogen flow and the biochar
222 and bio-oil were collected and weighed. The syngas (hydrogen, oxygen, nitrogen, carbon
223 monoxide, and dioxide, methane, ethane, and ethylene) was quantified using a micro-
224 chromatography device (Varian CP-4900, Agilent, Germany). The first column (CP-Sil CB)
225 was operated at 37 °C to separate the H₂ and the O₂, while the second column (Molsieve 5Å
226 PLO) was operated at 37 °C to separate the N₂, CO, and CH₄, and the third column (HayeSep
227 A) was operated at 35 °C to separate the CO₂, C₂H₂, C₂H₄, and C₂H₆. The gaseous compounds
228 were detected by a thermal conductivity detector. The injector and the detector temperatures
229 were 50 °C and 55 °C, respectively. The analyses of the syngas were carried out every 5
230 minutes during the pyrolysis reaction using the micro-GC. The mass of the produced syngas

231 M_{Syngas} (g) was determined by the difference between the output and input gas flow during the
232 pyrolysis process using an acquisition system linked to two flowmeters measuring the input
233 (flowmeter BROOKS) and the output (flowmeter M.M.T). Equation (1) was used to calculate
234 the mass of the syngas, as described below:

$$\begin{aligned} 235 & M_{\text{Syngas}}(g) \\ 236 & = \sum (\text{output flow (g/min)} - \text{input flow (g/min)})/122 \end{aligned} \quad (1)$$

237 where 122 is the number of acquisitions per min.

238 The biochar, bio-oil, and syngas product yield percentages were calculated as follows:

$$239 \quad \text{Biochar (wt\%)} = M_{\text{Biochar}}(g)/M_{\text{Solid digestate}}(g) \times 100 \quad (2)$$

$$240 \quad \text{Bio - oil (wt\%)} = M_{\text{Bio-oil}}(g)/M_{\text{Solid digestate}}(g) \times 100 \quad (3)$$

$$241 \quad \text{Syngas (wt\%)} = M_{\text{Syngas}}(g)/M_{\text{Solid digestate}}(g) \times 100 \quad (4)$$

242 where M_{Biochar} , $M_{\text{Bio-oil}}$, and M_{Syngas} represent the biochar, bio-oil, and syngas masses produced
243 during the pyrolysis, and $M_{\text{Solid digestate}}$ represents the mass of the solid digestate.

244 The losses during pyrolysis (approximately 6%) were considered to be the bio-oil trapped in
245 the walls of the cooling system, and they were taken into account in the bio-oil calculation.

246 The bio-oil obtained in this work was separated into two different phases: an organic phase
247 and an aqueous phase obtained by decantation using dichloromethane (99.8%, from Sigma-
248 Aldrich®) as the organic solvent. The weight and the yield were measured after decantation.

249 Anhydrous Na_2SO_4 was added to the solvent mixture/organic phase to remove residual water.

250 The solvent was then evaporated using a rotary evaporator, the organic phase of bio-oil was
251 weighed, and its yield was measured.

252 The average lower heating value (LHV) of the syngas was calculated based on Equation (5)

253 (Lv et al., 2004), assuming that the N_2 had been separated from the produced syngas. The

254 predictive higher heating value (HHV) (MJ/kg) of the organic phase of the bio-oil was
255 calculated using ultimate analysis in Equation (6) (Troy et al., 2013) as follows:

$$256 \quad LHV(MJ / Nm^3) = [30 \times v/v\% CO + 25.7 \times v/v\% H_2 + 85.4 \times v/v\% CH_4 + 151.3 \times$$
$$257 \quad \quad \quad v/v\% (C_2H_4 + C_2H_6)] \times 0.42] \quad (5)$$

$$258 \quad HHV (MJ/ kg) = [3.55 \times C^2 - 232 \times C - 2230 \times H + 51.2 \times (C \times H) + 131 \times N +$$
$$259 \quad 20,600]/1000 \quad (6)$$

260 **2.4 Analytical methods**

261 **2.4.1. Physicochemical analysis**

262 The Dry Matter (DM) and Volatile Solids (VS) contents in the organic wastes and the co-
263 products were determined according to the protocol outlined by the American Public Health
264 Association (APHA, 2005). The pH of the digestate was determined using a WTW 340i
265 reference pH meter. Ammonium (NH₄⁺) was determined using reagent kits (Spectroquant[®],
266 Germany) for NH₄⁺ by spectrophotometry (photoLab[®] S6, WTW, Germany). To determine
267 the concentration of the VFAs, the digestate was centrifuged for 20 minutes at 9,600 rpm
268 using a centrifuge system (Hettich Zentrifugen, Rotanta 460) to recover the liquid fraction. An
269 internal standard solution was prepared from 1 g of ethyl-2-butyric acid diluted in 1 L of
270 water acidified with 2.5% phosphoric acid. A 1 mL aliquot of internal standard solution was
271 then added to 2 mL of the liquid sample. The mixture was filtered using a 0.2- μ m nylon filter
272 attached to a syringe. The filtered liquid was introduced into a vial for analysis by a gas
273 chromatography system (GC-7890B) coupled to a flame ionization detector (FID). The
274 FOS/TAC (Free Organic Acids / Total Inorganic Carbonate) ratio, which corresponds to the
275 total acid and buffer capacity levels, was determined by acidification of the sample prepared
276 as 2 g of digestate diluted in 50 mL of deionized water under magnetic agitation with sulfuric
277 acid (0.1 N) from a graduated burette. A first acidification to a pH of 5.1 determines the
278 buffer capacity of the medium. A second acidification to a pH of 3.5 can quantify the amount
279 of total acids in the medium. The Chemical Oxygen Demand (COD) of the LD was analyzed

280 using commercial kits (Spectroquant[®], Merck, Germany). A 1 mL aliquot of centrifuged LD
281 was placed in the commercial tubes. The tubes were then heated to 148 °C in a preheated
282 thermoreactor for 120 min. Finally, the COD was measured by an automatic
283 spectrophotometer (photoLab[®] S6, WTW, Germany). The theoretical COD of the feedstocks
284 (wastewater sludge and quinoa residues) and the solid digestate were determined based on
285 CHNS analysis according to the method reported by Wei et al., (2018). For the COD balances
286 and biogas equivalence presented in **Fig. 2**, it was assumed that 1g of COD is equivalent to
287 1NmL of CH₄ (Im et al., 2020). The total Kjeldahl Nitrogen (TKN) content of the soil and the
288 LD was determined according to the Kjeldahl method (Kjeldahl, 1883) by using a
289 mineralizator (BUCHI digestion unit K-438) and a distillator/titrator (BUCHI K-370).
290 Moreover, the N-NH₄⁺ content of the LD was determined by the titrimetric method after
291 distillation using a BUCHI K-370 distillatory (Rodier, 1975).

292 A thermogravimetric analyzer (TGA 2-LF, Mettler Toledo[®], Switzerland) was used to assess
293 the thermal degradation of the solid digestate and the stability of its biochar, as well as to
294 determine the moisture, volatile matter, fixed carbon, and ash contents according to the
295 protocol reported in Tayibi et al., (2020b). The fibers (cellulose, hemicelluloses) and the
296 Klason lignin content of the dry solid digestate were determined using the NREL protocol
297 (Sluiter et al., 2008). Briefly, the Klason lignin content was determined as the weight of the
298 residues retained on a sintered glass crucible filter (Ø=25mm), and the soluble fractions were
299 analyzed by high-pressure liquid chromatography (HPLC) to quantify the monosaccharides
300 content (i.e., glucose, xylose, and arabinose). The HPLC (Alliance[®] HPLC System, Waters,
301 USA) analysis was performed using a column (Aminex[®] HPX-87H, BioRad, France) at 40 °C
302 and 0.3 mL/min of 0.005 M H₂SO₄. All of the measurements were performed in triplicate.
303 The cellulose and the hemicellulose percentages were determined by Equations (7) and (8),
304 respectively.

305 $Cellulose(\%) = [(Glucose(g/L) \times V_{tot})/M_{ini}] \times 100/1.11$ (7)

306 $Hemicelluloses (\%) = [(Xylose(g/L) + Arabinose(g/L) \times V_{tot})/M_{ini}] \times$
307 $100 /1.13$ (8)

308 where V_{tot} and M_{ini} represent the total volume of the hydrolysis medium (0.025 L) and the
309 initial mass of the sample in grams, respectively, while 1.11 represents the conversion factor
310 between glucose and cellulose and 1.13 represents the conversion factor between monomers
311 (xylose and arabinose) and hemicelluloses (Barakat et al., 2015).

312 The nutrient content (P, K, Mg, S, Ca, and Na) and the minor metallic content (Pb, Cd, Cu,
313 Ni, Hg, Zn, Cr, and As) were determined by inductively coupled plasma mass spectrometry
314 (ICP-MS) (X SERIES 2 ICP-MS, Thermo Fisher Scientific, USA) equipped with a cooled
315 spray chamber, a quadrupole mass spectrometer, and a collision cell. The ICP-MS settings
316 were as follows: a nebulizer flow of 0.82 L/min, an auxiliary flow of 0.80 L/min, a cool flow
317 of 13 L/min, a forward power of 1,400 Watts, and a cell gas He/H flow rate of 0.0045 L/min.
318 For this purpose, microwave-assisted mineralization of the solid digestate and its biochar was
319 performed after the addition of nitric acid (65%) and hydrogen peroxide (30%). The reaction
320 was conducted for 30 min at room temperature, and the mixtures were then placed in the
321 microwave reactor (flexiWAVE, Milestone, USA) and heated for 20 min to reach 210 °C,
322 which was maintained for 20 min and then cooled for 25 min. The obtained solutions were
323 filtered using 0.2- μ m filters and then analyzed by ICP-MS. The ultimate analyses (C, H, N, O,
324 and S) of the dry solid digestate, its biochar, and the organic phase of bio-oil and dry tomato
325 plants were determined in duplicate using an elemental analyzer (varioMicro V4.0.2,
326 Elementar[®], Germany).

327 **2.5 Agronomic tests**

328 **2.5.1. Carbon mineralization test**

329

330 The effect of biochar (25 tons/ha) on soil CO₂ emission with or without the addition of LD
 331 (170 kg N/ha) was explored by a 91-day indoor incubation experiment based on the AFNOR
 332 FD U44-163, (2018) standard. The biochar and the liquid digestate (LD) were added and
 333 mixed with the soil as follows: soil, soil + biochar (B25), soil + LD + biochar (B25), and soil
 334 + LD. Each condition was distributed into cups containing the equivalent of 25g of dry soil.
 335 These cups were then placed in hermetically sealed containers in the presence of sodium
 336 hydroxide and incubated at 28 °C. The humidity was kept constant throughout the experiment
 337 (equivalent to the field water retention capacity of pF 2.8). The carbon mineralized by the
 338 sample was measured after 1, 3, 7, 14, 21, 28, 49, 70, and 91 days of incubation by
 339 assessment of the C-CO₂ trapped in the sodium hydroxide (NaOH; 0.5 mol/L). This
 340 measurement was performed on three repeats. A mixture of sodium carbonate (Na₂CO₃) and
 341 sodium hydroxide was assayed. The carbonates were precipitated with an excess of barium
 342 chloride (BaCl₂; 20 wt%) solution. The sodium hydroxide that remained free was titrated with
 343 hydrochloric acid (HCl; 0.1 mol/L). Thymolphthalein (a 0.1% solution in ethanol) was used
 344 as the color indicator. The microbial respiration was calculated according to the following
 345 Equation (9):

$$\begin{aligned}
 346 \quad & \text{Microbial respiration} \left(\frac{mg(C - CO_2)}{kg \text{ dry soil}} \right) \\
 347 \quad & = 0.5 \times [(M_{NaOH}(mol/L) \times Vol_{NaOH}(L)) - (M_{HCl}(mol/L) \times Vol_{HCl \text{ used}}(L))] \\
 348 \quad & \times Mm_C \left(\frac{g}{mol} \right) \times 1000 / m_{soil}(kg) \quad (9)
 \end{aligned}$$

349 where, M_{NaOH} and M_{HCl} are the concentrations of the NaOH and the HCl solutions used in
 350 mol/L, respectively, Vol_{NaOH} is the volume of the NaOH solution, Vol_{HCl} is the volume of
 351 HCl used in the titration (L), Mm_C represents the molar mass of carbon (12.01 g/mol), and
 352 m_{soil} is the amount of soil in each condition (0.025 kg).

353 **2.5.2. Nitrogen mineralization test**

354 This test was also based on the AFNOR FD U44-163, (2018) standard. Biochar (25 tons/ha)
355 and LD (170 tons/ha) were added and mixed with the soil as follows: soil, soil + biochar
356 (B25), soil + LD + biochar (B25), and soil + LD. The experiment was carried out in soil cups
357 (25 g of dry soil). Ammonium (NH_4^+) and nitrate (NO_3^-) ions were extracted from three
358 repeats after 0, 7, 14, 28, 56, and 90 days of incubation at 28 °C with moisture maintenance
359 (pF 2.8). For each sampling date, a procedure to extract the mineral nitrogen contained in the
360 samples by mixing the soil with 100 mL of a KCl solution (1 mol/L) was carried out. The
361 samples were placed on a rotating agitation device for 1 hour (Heidolph, Reax 20, Germany).
362 The samples were then filtered using filter paper. The filtrate samples were frozen before
363 being sent to the laboratory for determination of the ammonia nitrogen levels as NH_4^+ and
364 ammonium nitrate. The measurement of NH_4 was performed according to the modified NF U
365 42-125, (1985) standard, while the measurement of NO_3 was performed by colorimetry
366 (Hood-Nowotny et al., 2010).

367 **2.5.3. Ammonia nitrogen volatilization (NH_3)**

368 The objective of this experiment was to estimate the loss of nitrogen by evaporation of
369 ammonia nitrogen (NH_3) related to the supply of LD (170 kg N/ha), with or without biochar at
370 25 tons/ha (B25), using a closed dynamic flow system. The following conditions were
371 investigated: soil, soil + biochar (B25), soil + LD + biochar (B25), and soil + LD. The altered
372 soils were incubated for 15 days and added at 183 g. All of the conditions were repeated four
373 times. To allow microbiological activity in each enclosure, distilled water was added to reach
374 60% of the soil retention capacity. Volatile ammonia nitrogen was captured in an acid trap.
375 The traps were changed eight times over the 15-day period to determine the kinetics of the
376 volatilization. The experimental system comprised three main parts: an incoming air condition
377 control system (consisting of a bottle of distilled water, a bottle of sulfuric acid, and a second

378 bottle of distilled water); a 500 mL closed volatile chamber containing the modified soil
379 (biochar with or without LD); and an acidic ammonia trapping system. The airflow was set to
380 600 L/h (1.25 L/min) at the chamber outlet. For each device, 9 samples were taken during this
381 test, at 1, 2, 3, 6, 8, 10, 13, and 15 days. The acid trap (0.05 mol/L sulfuric acid) provides the
382 protons needed to switch from gaseous NH_3 to NH_4^+ . The acid traps were assayed by
383 colorimetry to obtain the concentration of NH_4^+ in the volume of acid, thereby allowing
384 determination of the amount of NH_3 that had evaporated. These amounts were related to the
385 dry soil mass. The quantities were accumulated to determine the kinetics of the ammonia
386 nitrogen volatilization.

387 **2.5.4. Plant growth test**

388 The agronomic value of coupling biochar (at doses of 25 and 50 tons/ha) with LD (170 kg
389 N/ha) was evaluated by determining the growth parameters during the first vegetative stage
390 (relative seed germination and aerial dry biomass) using tomato as the plant model. Plant
391 experiments with tomato seeds were performed in small pots with a volume of 0.5 L placed in
392 a growth chamber (Fitotron®, Weiss Gallenkamp, UK) according to the OECD 208
393 guidelines (2006) under controlled conditions. The environmental conditions during the
394 testing were as follows: 16 h of light at 25 °C, 8 h of darkness at 18 °C, with 60% relative
395 humidity for the periods of light and 80% relative humidity during the periods of darkness.
396 Seven conditions were tested: soil alone; soil + industrial fertilizers using a mixture of DAP
397 and ammonium nitrate to reach an application of 170 kg N/ha of mineral nitrogen and 10 kg
398 P/ha of phosphorus (soil + IF); soil with LD applied at 170 kg N/ha (soil +LD); soil with LD
399 and biochar application at 25 tons/ha (Soil + LD + B25); soil with LD and biochar application
400 at 50 tons/ha (Soil + LD + B50); soil with biochar application at 25 tons/ha (soil + B25), and
401 soil with biochar application at 50 tons/ha (soil + B50). The mixture for each condition was
402 prepared at 70% of the water retention of soil. Six seeds were planted in each pot, using four

403 replicates for each condition. Each pot was manually sub-irrigated every 48 h by the addition
404 of water to reach the initial weight. After 70% germination of the control, two germinated
405 seeds were removed and four were kept for the growing period. After 41 days, the plants were
406 harvested by cutting them at ground level and they were then dried in an oven at 70 °C for 24
407 h. For each condition, the relative seed germination expressed as the percentage according to
408 Equation (9) and the aerial dry biomass expressed in (g DM/100 plants) was determined
409 according to Equation (10). Generally, a relative seed germination above 70% indicates low
410 phytotoxicity.

411 Relative Seed Germination (%)

$$412 \quad = (\text{Mean of germinated seed} / \text{Initial number of seeds}) \times 100 \quad (9)$$

$$413 \quad \text{Aerial dry biomass (g DM/ 100 plants)} = (M_{\text{dry (70 °C)}} / 4) \times 100 \quad (10)$$

414 where $M_{\text{dry (70 °C)}}$ represents the mean of the aerial dry biomass (g DM) for each condition and
415 4 is the number of plants in each pot at harvesting time.

416 To compare the different conditions tested, the analysis of variance (ANOVA) method was
417 used to analyze the impact of the various fertilization modes, and the confidence level
418 considered was 95%.

419 **3. Results and Discussion**

420 **3.1. Anaerobic digestion**

421 In the first instance, anaerobic co-digestion of wastewater sludge and quinoa residues was
422 investigated in mesophilic CSTR anaerobic digesters. The main physicochemical properties of
423 the quinoa residues and the wastewater sludge are reported in **Table 1**. The quinoa residues
424 were composed of 24.6%DM of cellulose, 14.1 %DM of hemicelluloses, and 7.0 %DM of
425 lignin. The quinoa residues had a low nitrogen content of 0.21%DM and a high C/N ratio of
426 216. All of these values are in agreement with what has previously been reported for
427 lignocellulosic biomass in the literature (Monlau et al., 2013). By contrast, the wastewater

428 sludge had a higher nitrogen content of 7.0%DM and a lower C/N ratio of 5.8. Interestingly,
429 co-digestion of quinoa residues and wastewater sludge in the AD process resulted in a C/N
430 ratio of 13, which is more in agreement with the C/N ratios that have been reported to be
431 optimal for the AD process, with values ranging from 15 to 30 (Morales-Polo et al., 2018;
432 Van et al., 2020).

433 First of all, biochemical methane potential tests were carried out, and a value of 236 ± 2 NL
434 $\text{CH}_4/\text{kg VS}$ was determined for the wastewater sludge and 237 ± 2 NL $\text{CH}_4/\text{kg VS}$ for the
435 quinoa residues (data not shown). In this study, quinoa and wastewater sludge exhibited
436 similar methane potentials and such values are in agreement with previous studies that
437 investigated methane potential of lignocellulosic biomass (Monlau et al., 2012) and
438 wastewater sludge (Elbeshbishy et al., 2012). Monlau et al. (2012) have reported methane
439 potential ranging from 155 NL $\text{CH}_4/\text{kg TS}$ to 300 NL $\text{CH}_4/\text{kg TS}$ for various lignocellulosic
440 biomasses. In parallel, co-digestion of quinoa residues and wastewater sludge (at 57.5/42.5%
441 VS) resulted in a methane potential of 237 NL $\text{CH}_4/\text{kg VS}$ demonstrating that the co-digestion
442 did not exhibit positive synergy at BMP scale which has been previously reported in literature
443 as the synergy effect depends on the biomass that are co-digested but also on the inoculum
444 initially used (Elalami et al., 2019; Kim et al., 2019).

445 Then, co-digestion of quinoa residues and wastewater sludge was simulated for 16 weeks
446 (corresponding to approximately three hydraulic retention times (HRTs) of 38 days) in
447 mesophilic CSTR digesters, as shown in **Fig. 1A**. These durations are thought to be the
448 minimum to assess the stability of the AD process (Sambusiti et al., 2013). After an increase
449 of the organic loading rate during the two first weeks, the OLR was further set at 2 kg
450 $\text{VS}/\text{m}^3/\text{day}$. During the overall period of the assay, the pH remained stable around 7.4 and the
451 temperature was 38 ± 2 °C. All of the values presented below are averages of the values of the
452 last HRTs (3rd HRT).

453 The concentration of ammonium remained below 2.5 gN-NH₄/L, and no specific inhibition
454 was observed in terms of methane production. The threshold inhibition level for total
455 ammonia nitrogen reported in the literature varies from 1.5 to 2.5 g/L (Jiang et al., 2019;
456 Sambusiti et al., 2013; Yenigün and Demirel, 2013), but after inoculum acclimation
457 concentrations up to 2.5 g/L can be reach inside the anaerobic digester (Jiang et al., 2019).
458 The total ammonia nitrogen (TAN), which is generally defined as the sum of free ammonia
459 nitrogen (FAN, NH₃-N) and ammonium nitrogen (NH₄⁺-N), is generated during the
460 hydrolysis of proteins, urea, and nucleic acids (Morozova et al., 2020). The content of VFAs
461 (data not shown) remained lower than 0.1 g_{eq.acetate}/L throughout the assay, thus demonstrating
462 good stability of the process and no acidification. These results were also reflected by the
463 FOS/TAC ratio (**Fig. 1B**), which was below the safety threshold value of 0.3 (Sambusiti et al.,
464 2013). To assess the performances and to identify the absence of inhibition, the average
465 specific methane yield was computed from the slope of the trend line fitting the data of the
466 cumulative methane production versus the cumulative VS fed to each reactor. As can be seen
467 in **Fig. 1C**, the final specific methane production was 238 NL CH₄/kg VS, corresponding to
468 100% of the result obtained by the biochemical methane potential (BMP) batch tests. These
469 observations are in agreement with previous studies that investigated the methane production
470 of organic wastes on a pilot scale (Sambusiti et al., 2013). In a previous study, Alagöz and
471 Yenigün, (2015) investigated mesophilic co-digestion of olive residue and waste activated
472 sludge, and they reported a methane potential of 210 NL CH₄/kg VS. Similarly, Li et al.
473 (2017) investigated mesophilic anaerobic co-digestion of waste activated sludge with tobacco
474 residues, and they reported a methane potential of 181 to 204 NL CH₄ /kg VS depending on
475 the substrate ratio. Finally, COD (chemical oxygen demand) balances were performed in
476 parallel on the overall AD system to monitor the absence of losses and closure of the organic
477 matter cycles. The balances are presented in **Fig. 2**. The COD recovery in the output (sum of

478 the COD of biogas, liquid and solid digestate) was equivalent to 95% of the COD of the input,
479 thus demonstrating that the matter fluxes are well evaluated and identified. At the end of the
480 3rd HRT, the digestate was separated into a liquid and a solid fraction by a wine press, and the
481 solid fraction was oven-dried. Pyrolysis of the solid digestate was investigated in the next
482 section.

483 3.2. Pyrolysis

484 Pyrolysis was carried out on the solid fraction of the digestate at 500 °C for 1 h after drying of
485 the solid digestate. The pyrolysis products distribution was as follows: 40 ± 1.2 wt% biochar,
486 35.8 ± 2.9 wt% bio-oil, and 23.7 ± 4.9 wt% syngas. The syngas produced during the pyrolysis
487 process was analyzed and the distribution of the syngas compounds is presented in **Fig.3**. The
488 LHV of the syngas was 11.8 MJ/Nm^3 , which is in agreement with previously reported values
489 ranging from 12.9 MJ/Nm^3 to 15.7 MJ /N m^3 (Monlau et al., 2015b; Neumann et al., 2015;
490 Tayibi et al., 2021). The syngas mainly consisted of CO₂, CH₄, CO, and H₂, with a small
491 amount of C₂H₄, C₂H₆, and C₂H₂. The production of CO₂ and CO was mostly due to
492 decarboxylation and decarbonylation reactions (Jęczmionek and Porzycka-Semczuk, 2014).
493 The high content of CO₂ can also result from the cracking of remaining fibers such as
494 cellulose and hemicelluloses in the solid digestate fraction (Liu et al., 2011). In a recent study,
495 Ghysels et al. (2020) reported a similar composition of syngas from cocoa wastes after
496 pyrolysis at 500 °C. Indeed, on an N₂-free basis, the dominant compound in this stream was
497 carbon dioxide, at a concentration of 79.5 vol% for pyrolysis at 500 °C, and CO, CH₄, and H₂
498 were also present at concentrations of 13.2 vol%, 3.9 vol%, and 2.5 vol%, respectively.

499 In parallel to syngas, bio-oil was also generated during the pyrolysis process. At industrial
500 level, bio-oil separation by solvent seems to be a promising option with an organic phase that
501 can be used as a fuel or building blocks (Hossain et al., 2016; Pütün et al., 2005), whereas the
502 aqueous phase can be recirculated as feedstock for the AD process (Torri and Fabbri, 2014).

503 Hossain et al. (2016) have recently demonstrated the feasibility in an engine combustion of
504 using organic oil from solid digestate pyrolysis in blend with waste cooking oil and butanol.
505 In our study, the bio-oil obtained was separated into an organic and aqueous phase, at a ratio
506 of 23.1 wt%, and 76.9 wt%, respectively. Similarly, Ghysels et al. (2020) reported a ratio of
507 organic and aqueous phases of 25% and 75%, respectively, after pyrolysis of solid digestate
508 derived from cocoa wastes at 500 °C, which is in agreement with our study. The main
509 physicochemical properties of the organic phase of the bio-oil are summarized in **Table 2**.
510 The organic phase of the bio-oil had a high carbon content (70.5 wt%) and a low oxygen
511 content (14.9 wt%), which is required for bio-oil fuel applications. The higher heating value
512 (HHV) of the organic phase of the bio-oil (**Table 2**) was estimated to be 33.9 MJ/kg. This
513 HHV of bio-oil is higher than that reported by Opatokun et al. (2015) from food digestate
514 pyrolyzed at 500 °C with a calorific value of 13.5 MJ/kg, but in their case all the bio-oil was
515 considered and not only the organic phase. Nonetheless, our value was in the same range as
516 the value of 29.7 MJ/kg reported by Ghysels et al. (2020) after pyrolysis at 500 °C of solid
517 digestate from the anaerobic digestion of cocoa wastes. Generally, the organic phases from
518 bio-oil after pyrolysis of solid digestate at 500 °C have been reported to be dominated by
519 phenolic compounds (Ghysels et al., 2020; Tayibi et al., 2020a; Wei et al., 2018). For
520 instance, Wei et al. (2018) reported that the content of phenolic compounds was 70.4% in the
521 OP of the bio-oil produced from digestate (originating from sargassum anaerobic digestion)
522 pyrolyzed at 450 °C (Wei et al., 2018).

523 Finally, a third product was generated during the pyrolysis process (at 40 wt%), as a
524 carbonaceous material called biochar. Similarly, Opatokun et al. (2017) reported biochar
525 yields from 25 to 61%wt after pyrolysis at temperatures ranging from 300 °C to 700 °C of
526 solid digestate from anaerobic digestion of food wastes. Similarly, Neumann et al. (2015)
527 reported a biochar yield of 36%wt after pyrolysis at 500 °C of solid anaerobic digestate. The

528 produced biochar was characterized, and their main physicochemical properties are reported
529 in **Table 3** and compared to the EBC (European Biochar Certificate) and IBI (International
530 Biochar Initiative). The carbon content of the biochar was 47.2 wt%, indicating that it is a
531 class 2 biochar according to the IBI and that it is considered a bio carbon mineral (BCM) and
532 not a biochar according to the EBC (**Table 3**). Compared to the solid digestate, the amount of
533 O and H decreased in the biochar due to the decarboxylation and dehydration reactions during
534 the pyrolysis process. The ash content of the biochar was 38.2 wt% compared to only 15.9
535 wt% in the solid digestate (**Table 3**). The relatively high ash content in the solid digestate can
536 be attributed to the fact that during the AD process the microorganisms convert the organic
537 fraction of the organics into CO₂ and CH₄ (Monlau et al., 2015a), resulting in a higher
538 concentration of inorganics in the digestate than in the original feedstocks. Macronutrients
539 (i.e., N, P, K, Mg, and Ca) were also analyzed in the solid digestate and the respective
540 biochar. Except for N, all the macronutrients were enriched in the biochar, which is in
541 agreement with previous publications that investigated biochar production from solid
542 digestate (Calamai et al., 2019; Monlau et al., 2016). Minor metals (i.e., Pb, Cd, Cu, Ni, Hg,
543 Zn, Cr, and As) were also analyzed in the biochar. All of the values obtained were lower than
544 the maximal threshold levels recommended by the IBI (International Biochar Initiative).
545 Nonetheless, most of the values were higher than the threshold levels recommended by the
546 EBC (European Biochar Certificate), except for Hg, as shown in **Table 3**.

547 **3.3. Agronomic potential of coupling biochar and LD**

548 **3.3.1. Plant growth tests on tomato plants**

549 The impact of biochar (at 25 and 50 tons/ha) on the growth of tomatoes was investigated
550 during the first vegetative stage of the plants. The biochar concentration was chosen based on
551 the data in the literature (Glaser et al., 2015; Greenberg et al., 2019). Biochar has recently
552 been shown to be of considerable relevance to sustainable agriculture (Mandal et al., 2020;

553 Semida et al., 2019), even though biochar does not have any fertilizing actions and should
554 generally be added with a fertilizer (Greenberg et al., 2019; Ronga et al., 2020; Tayibi et al.,
555 2021). Since biochar does not provide an adequate supply of nutrients to serve as the sole
556 source of fertilization, combined effects with the LD (applied at 170 kg N/ha) were evaluated
557 on the relative seed germination and the aerial dry biomass of tomatoes. The liquid digestate
558 was composed of 3.8 wt% dry matter, 2.4 wt% volatile matter, 0.37 wt% total Kjeldahl
559 nitrogen (TKN), 0.15 wt% ammonium (NH_4^+), 0.27 wt% potassium (K_2O), and 0.25 wt%
560 phosphorus (P_2O_5).

561 Seed germination is a relevant indicator of potential phytotoxicity. LD added alone did not
562 affect the relative seed germination with 88 (± 8) % in comparison to soil alone (92 (± 9) %).
563 Interestingly, biochar addition at 25 and 50 tons/ha did not exhibit a negative impact on the
564 germination rate in comparison with soil alone and soil with industrial fertilizers, as shown in
565 **Fig. 4**. Indeed, relative seed germination of 92 (± 9) %, 83 (± 16) %, 79 (± 8) % were reported
566 for soil alone, soil with 20 tons and 50 tons of biochar, respectively. Similarly, Bu et al.
567 (2020) investigated the effect of rice husk and woodchip biochar at various application rates
568 (1%, 2%, and 5% by weight) on seed germination of *Robinia pseudoacacia* in calcareous soil,
569 and they did not find that there was a negative impact (Bu et al., 2020). Furthermore, the
570 combination of LD and biochar did not exhibit a negative impact on germination in
571 comparison with soil alone and soil with industrial fertilizers. These results are also in
572 agreement with those of Tayibi et al. (2020a), who similarly did not observe a negative impact
573 on the germination of wheat when biochar (at 50 tons/ha) was added in combination with LD.

574 In parallel, the growth efficiency of tomato plants when the soil was amended by biochar (at
575 25 and 50 tons/ha) in combination with LD was also investigated during the first vegetative
576 growth stage (41 days). As shown in **Fig. 4**, all the conditions tested resulted in higher aerial
577 dry biomass production than the soil alone. More specifically, the application of LD increased

578 the aerial dry biomass to 18 gDM/100 plants compared to unamended soil (11.6 gDM/100
579 plants), although it was slightly lower than with industrial fertilizers (20.8 gDM/100 plants).
580 These results confirm the ability of LD to improve plant growth as previously demonstrated
581 (Elalami et al., 2020; Nkoa, 2014; Solé-Bundó et al., 2017). A higher aerial dry biomass was
582 obtained for the condition that combined biochar and LD, with an increase of 33% compared
583 to soil amended with biochar alone (ANOVA test: $p < 0.05$) and an increase of 88%
584 compared to soil only (ANOVA test: $p < 0.05$). In parallel, the dry biomass obtained for the
585 condition combining soil and LD was lower by 13.8% compared to the soil treated with
586 industrial fertilizers, although the results were not significantly different according to the
587 ANOVA test ($p = 0.18$)

588 Adding biochar with LD increased the dry biomass by 4.5% and 7.9% for 25 tons/ha and 50
589 tons/ha, respectively, compared to soil fertilized with industrial fertilizers, which shows the
590 positive effect of coupling biochar and LD.

591 Ronga et al. (2020) also assessed the effect of digestate and biochar fertilizers on the yield and
592 fruit quality of tomatoes grown in an organic farming system, and they obtained similar
593 results. Indeed, they demonstrated that plants fertilized with LD and biochar had the
594 maximum marketable yield (72 tons/ha), followed by BC (67 tons/ha), and LD (59 tons/ha);
595 while the lowest production (47 tons/ha) was recorded with unfertilized plants. These results
596 are in agreement with Glaser et al. (2015), who reported a positive effect on maize silage by
597 combining digestate with biochar. Glaser et al. (2015) demonstrated that the application of
598 biochar-digestate (at a biochar rate of 1 and 40 tons/ha and digestate at 200 kg N /ha) to maize
599 increased the yields and plant nutrition compared to pure digestate. Interestingly, at a
600 concentration of 40 tons/ha of biochar, the co-application of digestate with biochar
601 significantly increased the maize yield by 42% compared to untreated plants without biochar
602 addition (Glaser et al., 2015). Greenberg et al. (2019) also investigated the effect of coupling

603 LD with biochar added at 2 and 40 tons/ha on *Zea mays*. For both biochar applications, there
604 were no significant differences in terms of the rye above-ground biomass. Nonetheless, such
605 experiments must be extended in the future at a field-scale, and several parameters should be
606 carefully investigated such as the nature and the quantity of biochar, the digestate origin and
607 properties, the type of the soil, and climatic conditions.

608 **3.3.2. Ammonia volatilization, C and N mineralization**

609 In light of the results obtained with tomato plant growth during the first vegetative stage, the
610 effect of coupling LD with biochar at a dose of 25 tons/ha on other agronomic parameters
611 (*e.g.*, ammonia volatilization, C and N mineralization) was investigated. The addition of
612 biochar on the C mineralization compared with the control (soil alone) was investigated first,
613 as shown in **Fig. 5A**. A slight but non-significant reduction of C mineralization was observed
614 in the presence of biochar compared to the control (soil alone). Carbon dioxide is generally
615 released by microbial decay of residual organic matter (Semida et al., 2019). These results
616 confirm the capacity of biochar to sequester C in soils and to contribute to carbon
617 sequestration (Clough et al., 2013; Semida et al., 2019). Bruun and EL-Zehery, (2012)
618 investigated the effect of biochar addition to soil amended by barley straw. Without biochar,
619 $48 \pm 0.2\%$ of the straw carbon was mineralized during the 451 days of the experiment. In
620 comparison, $45 \pm 1.6\%$ of C was mineralized after biochar addition at 1.5 g kg^{-1} . Similarly,
621 Yoo and Kang, (2012) demonstrated that the addition of biochar (at 2 wt%) in silt loam soils
622 did not affect the C mineralization compared with the soil alone. Fidel et al. (2019) also
623 investigated the impact of biochar (derived from wood) added at 0.5 wt%/wt% of silt soil on
624 CO_2 mineralization at different temperatures and humidity. They did not observe any
625 significant differences for any of the conditions between the CO_2 mineralization in the
626 biochar-amended soil and the unamended soil. The soil sequestration capacity of biochar
627 appears to depend on the soil typology, the climatic conditions, and the biochar origin

628 (Semida et al., 2019; Yoo and Kang, 2012). The addition of LD to the soil led to an
629 enhancement of the C mineralization due to the presence of soluble organic carbon that is
630 mineralized and NH_4^+ , and the C mineralization rate was determined to be 1,517 mg C-
631 CO_2/kg dry soil. Finally, as shown in **Fig. 5A**, the combination of biochar and LD led to
632 equivalent C mineralization compared to soil amended with LD only, and a net C
633 mineralization of 1,539 mg C- CO_2/kg dry soil. Aside from potentially sequestering carbon,
634 the impact of biochar added alone or in combination with LD on the N dynamics by
635 performing N mineralization experiments was also investigated. The addition of biochar did
636 not appear to affect the N mineralization dynamics compared to soil alone, as shown in **Fig.**
637 **5B**. These results confirm that, aside from a high biochar C/N ratio of 17 that can further
638 increase the C/N of soil, no N immobilization was noted, thus suggesting that biochar is
639 composed of recalcitrant organic carbon (Semida et al., 2019). Furthermore, the absence of N
640 mineralization enhancement after biochar application can be explained by the biochar
641 capacity to absorb NH_4^+ and NO_3^- that masks N mineralization or by the low amount of
642 hydrolyzable organic N forms in biochar (Ameloot et al., 2015; Clough et al., 2013). The
643 same tendency was observed in the presence of LD, as shown in **Fig. 5B**, demonstrating that
644 the biochar did not affect the microbial population involved in N mineralization. The increase
645 in N mineralization was 129-135 mg $\text{N}_{\text{mineral}}/\text{kg}$ dry soil.

646 The impact of coupling LD and biochar was also investigated in regard to ammonia
647 volatilization, as shown in **Fig. 5C**. Interestingly, the addition of biochar alone at 25 tons/ha
648 did not have any influence on the ammonia volatilization compared to soil alone. The addition
649 of digestate to the soil led to an increase of the ammonia volatilization of 1.8 mg N/kg dry soil
650 versus 0.4 mg N/kg dry soil for the non-amended soil. This increase of 1.8 mg N/kg dry soil
651 corresponded to 3.5% of the total nitrogen provided by the LD. This ammonia volatilization is
652 due to the presence of ammoniacal nitrogen present in the digestate that became volatilized

653 once applied in the soil (Nkoa, 2014; Plaimart et al., 2021). Similarly, Plaimart et al. (2021)
654 have reported that approximately 4.8% of the nitrogen was evaporated in the form of
655 ammonia after the application of digestate on a clay loam soil. Surprisingly, the co-application
656 of biochar and LD enhanced the ammonia volatilization by as much as 3 mg N/kg dry soil,
657 which can be explained by the fact that the alkaline nature of biochar added to soil promotes
658 ammonia volatilization (Sha et al., 2019). Such value of ammonia volatilization corresponded
659 to 5.8% of the total nitrogen initially provided and consequently biochar addition
660 simultaneously with LD resulted in 66% more N loss than LD application alone. Similar as
661 well as contradictory results have been observed in the literature, and the impact of biochar
662 addition on ammonia volatilization appears to depend on several parameters such as the
663 nature of the soil, the origin of the biochar, and the experimental conditions (Plaimart et al.,
664 2021; Sha et al., 2019).

665 **4. Conclusions**

666 In this study, an original cascading biorefinery approach that coupled AD and pyrolysis was
667 investigated for the valorization of organic wastes. AD led to a methane production of 219
668 NL CH₄/kg VS, and the organic phase (OP) of bio-oil and syngas from subsequent pyrolysis
669 of the solid digestate exhibited higher and lower heating values of 34 MJ/kg and 11.8
670 MJ/Nm³, respectively. Specific attention was paid to combining biochar and anaerobic LD
671 for agronomic purposes. The characteristics of the biochar were in accordance with the IBI
672 recommendations for soil amendment. The co-application of biochar with LD significantly
673 increased the ammonia volatilization by 64% compared to LD application alone. Although
674 co-application of biochar with LD did not impact the C and N mineralization, their
675 simultaneous use improved the growth of tomato plants up to 25% compared to LD
676 application alone.

677 **Acknowledgments**

678 The authors wish to thank the Cherifian Office for Phosphates (OCP group) for funding the
679 ATCLASS project.
680

681 **Table and Figure Captions:**

682 **Table 1.** The main chemical constituents of the feedstocks introduced into the anaerobic lab-
683 scale CSTR digester.

684 **Table 2.** The properties of the organic phase of bio-oil from the pyrolysis of the solid
685 digestate.

686 **Table 3.** The physicochemical properties of the solid digestate and the produced biochar
687 compared to the IBI (International Biochar Initiative) and the EBC (European Biochar
688 Certificate) recommendations.

689 **Fig.1.** (A) Organic loading rate effect, temperature, and pH changes during the AD process;
690 (B) Biomethane production and change in the NH_4^+ concentration during the AD; (C)
691 Cumulative biogas and methane production during the AD process vs. the cumulative VS
692 added.

693 **Fig.2.** Chemical oxygen demand (COD) mass balances of the AD CSTR process with quinoa
694 residues and wastewater sludge co-digestion.

695 **Fig.3.** Syngas distribution during the pyrolysis experimentation according to the temperature
696 process. Overall syngas composition produced during the pyrolysis process of solid digestate
697 are provided in the insert table.

698 **Fig.4.** Relative seed germination (%) and aerial dry biomass (gTS/100 plants) of tomato
699 plants.

700 **Fig.5.** (A) Microbial respiration, (B) Total nitrogen mineralization over time (from 0 to 91
701 days), and (C) Ammonia volatilization for the four conditions: soil, soil with biochar (at 25
702 tons/ha), soil with liquid digestate (LD), and soil with liquid digestate (LD) and biochar at 25
703 tons/ha (B25).

704

705

706 **Table 1.** The main chemical constituents of the feedstocks introduced into the anaerobic lab-
707 scale CSTR digester.

708

Parameter (units)	<i>Quinoa residues</i>	<i>Wastewater sludge</i>
DM (wt% FM)	90.1 ± 0.1	18.7 ± 0.1
VS (wt% DM)	88.9 ± 0.3	79.6 ± 2.2
C (wt%)	43.3 ± 0.2	41.2 ± 0.2
H (wt%)	6.0 ± 0.1	6.2 ± 0.2
N (wt%)	0.2 ± 0.0	7.0 ± 0.2
S (wt%)	0.1 ± 0.0	0.6 ± 0.0
O^a (wt%)	40.5 ± 0.3	41.2 ± 0.5
Cellulose (wt%)	24.6 ± 0.4	-

Hemicelluloses (wt%)	14.1 ± 0.5	-
Klason lignin (wt%)	7.0 ± 0.3	-
Ash (wt%)	10.0 ± 0.2	3.8 ± 0.4

^a $O\% = 100\% - C\% - H\% - N\% - S\% - Ash\%$

Parameters (units)	Solid digestate	Biochar	IBI standards V2.0	EBC standards V4.8
--------------------	-----------------	---------	--------------------	--------------------

709

710 **Table 2.** The properties of the organic phase of the bio-oil from pyrolysis of the solid
711 digestate.

712

Parameter (units)	Organic phase of bio-oil	713
C (wt%)	70.6 ± 0.9	714
H (wt%)	8.1 ± 0.7	715
N (wt%)	5.6 ± 0.5	716
S (wt%)	0.8 ± 0.1	716
O (wt%)^a	14.9 ± 1.0	717
HHV (MJ/kg)	33.9	718
Density (kg/L)	1.1	718
^a determined by difference		719

720

721

722

723

724

725

726

727

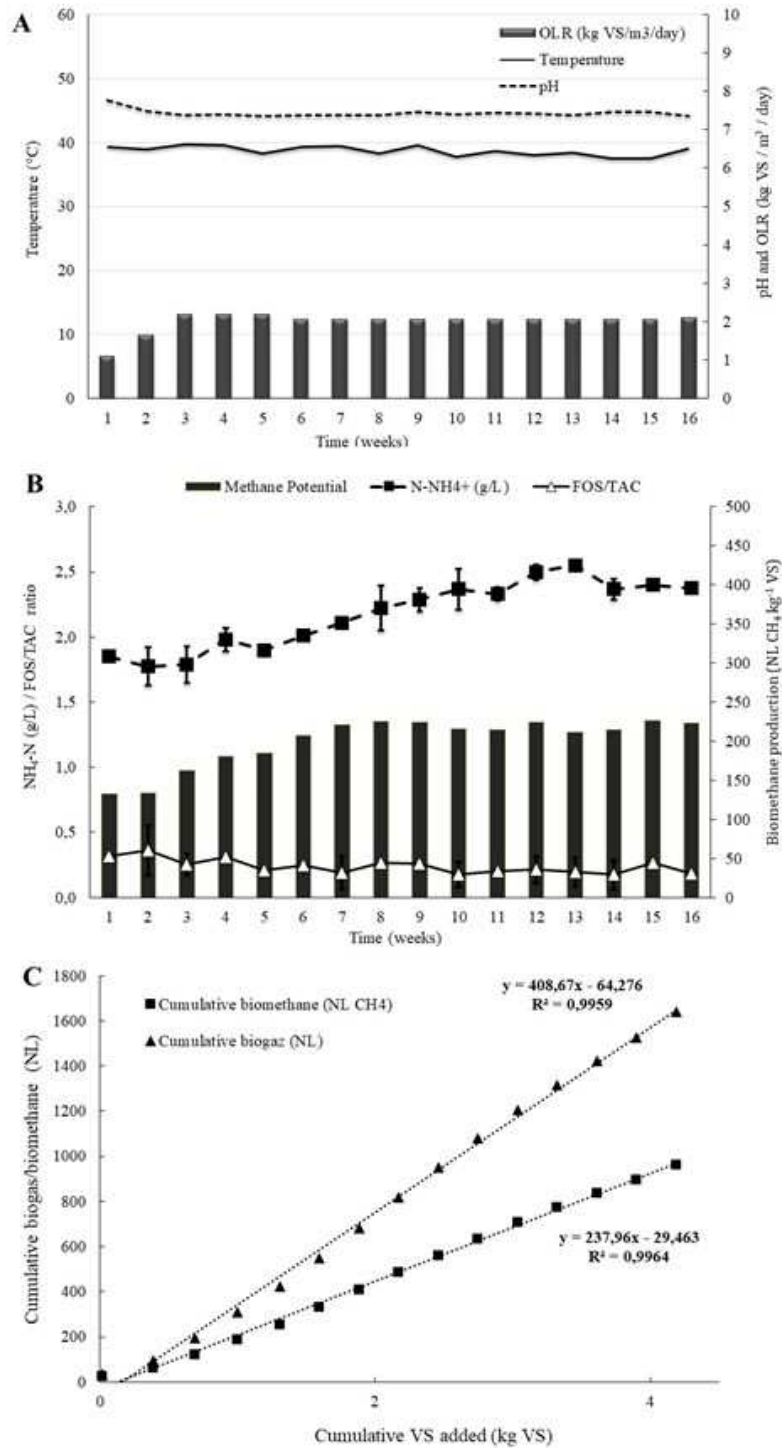
728 **Table 3.** The physicochemical properties of the solid digestate and the produced biochar
729 compared to the IBI (International Biochar Initiative) and the EBC (European Biochar
730 Certificate) recommendations.

pH	7.7 ± 0.02	9.8 ± 0.06	-	-
C (wt%)	37.0 ± 2.0	47.2 ± 5.3	10 wt% Minimum •Class 1: ≥ 60wt% •Class 2: ≥ 30wt% and ≤ 60wt%. •Class 3: ≥ 10wt% and ≤ 30wt%.	Biochar ≥ 50wt% Bio Carbon Minerals (BMC) < 50wt%
H (wt%)	4.6 ± 0.4	1.6 ± 0.1	-	-
N (wt%)	2.8 ± 0.6	2.8 ± 0.2	-	-
S (wt%)	0.6 ± 0.1	0.4 ± 0.1	-	-
O^a (wt%)	39.1 ± 1.7	9.7 ± 5.2	-	-
K (wt%)	1.3	3.1	-	-
P (wt%)	1.7	3.4	-	-
Mg (wt%)	0.4	0.6	-	-
Fe (wt%)	0.5	0.9	-	-
Ca (wt%)	1.7	3.6	-	-
Na (wt%)	0.2	0.4	-	-
H/C	0.13 ± 0.0	0.03 ± 0.0	-	-
O/C	1.06 ± 0.1	0.22 ± 0.13	-	-
Moisture (wt%)	8.3 ± 1.2	4.9 ± 1.3	-	-
Volatile matter (wt%)	60.4 ± 0.6	19.0 ± 0.7	Optional	Required
Fixed carbon (wt%)	15.8 ± 0.7	43.0 ± 0.0	-	-
Ash (wt%)	15.9 ± 1.2	38.2 ± 5.7	Required	Required
Cellulose (wt%)	17.8 ± 1.1	-	-	-
Hemicelluloses (wt%)	5.5 ± 0.0	-	-	-
Lignin (wt%)	18.3 ± 0.6	-	-	-
Minor metallic (mg/kg DM)				
Pb	28	54	70 - 500	< 150
Cd	2.8	5.2	1.4 - 39	< 1.5
Cu	220	389	63 - 1500	< 100
Ni	40	73	47 - 600	< 50
Hg	0.05	< 0.05	1 - 17	< 1
Zn	516	989	200 - 7000	< 400
Cr	120	209	64 - 1200	< 90
As	2.9	4.1	12 - 100	-

^aO% = 100% - C% - H% - N% - S% - Ash%

731

732



733

734 **Fig.1.** (A) Organic loading rate effect, temperature, and pH changes during the AD process;

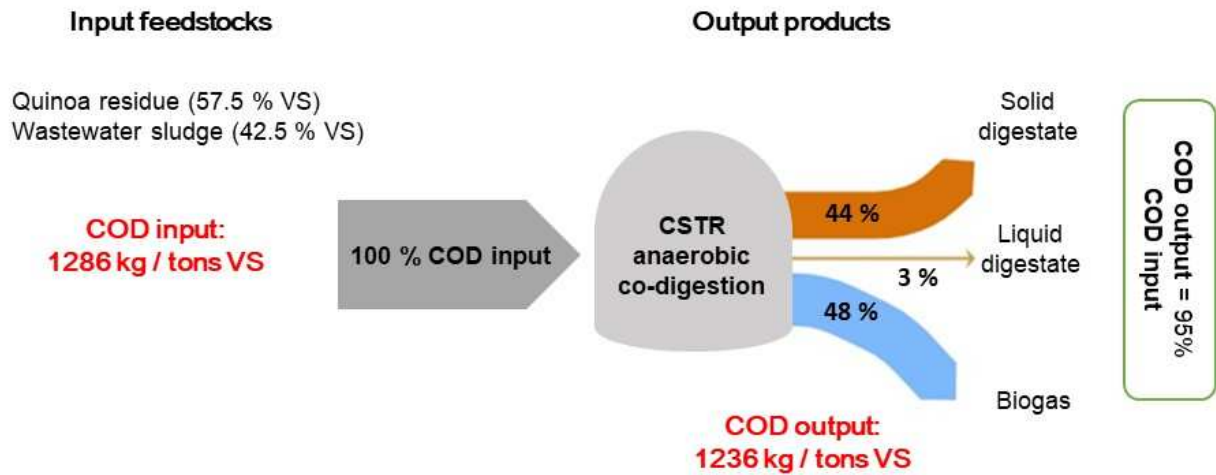
735 (B) Biomethane production and change in the NH₄⁺ concentration during the AD; (C)

736 Cumulative biogas and methane production during the AD process vs. the cumulative VS

737

added.

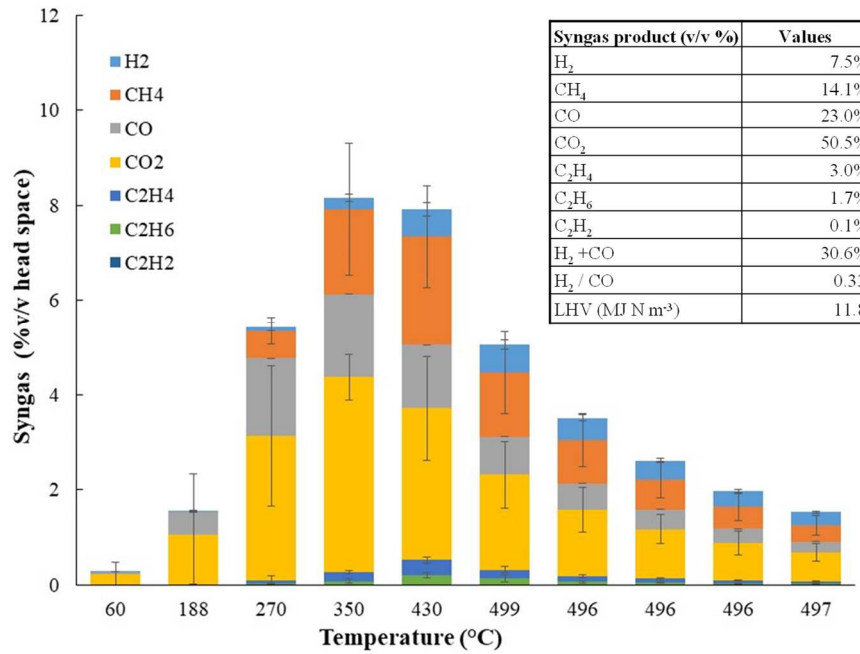
738



739

740 **Fig.2.** Chemical oxygen demand (COD) mass balances of the AD CSTR process with quinoa
741 residues and wastewater sludge co-digestion.

742

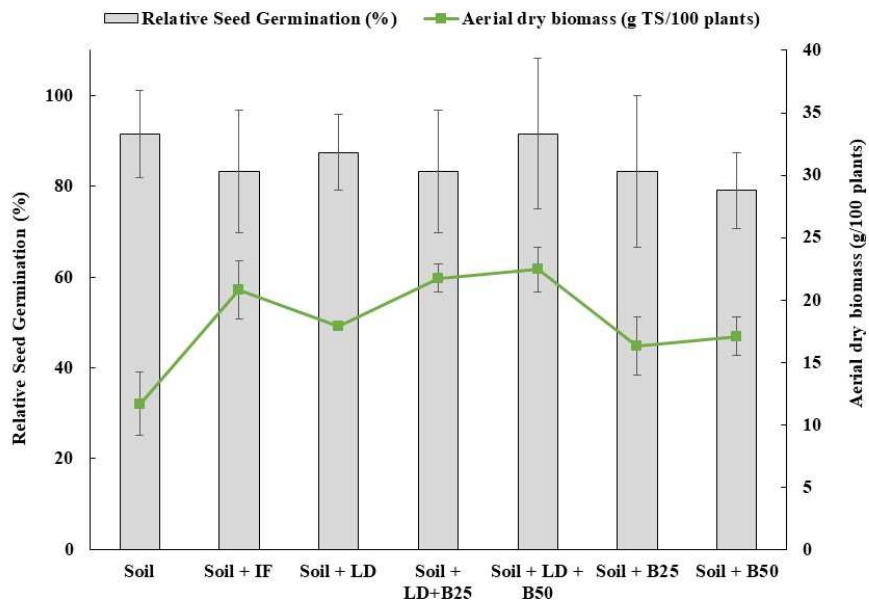


743

744

745 **Fig.3.** Syngas distribution during the pyrolysis experimentation according to the temperature
746 process. Overall syngas composition produced during the pyrolysis process of solid digestate
747 are provided in the insert table.

748

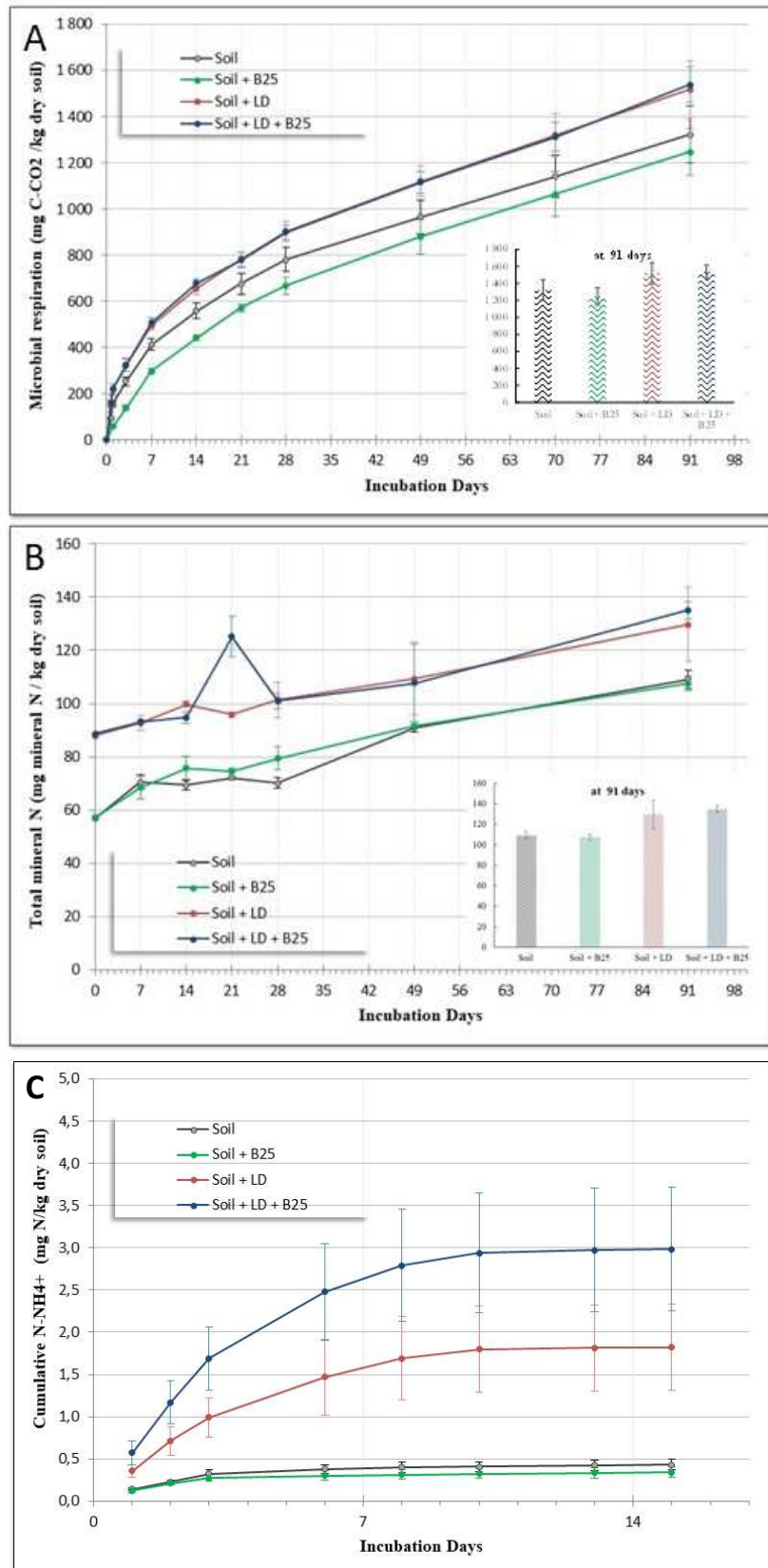


749

750

751

Fig.4. Relative seed germination (%) and aerial dry biomass (gDM/100 plants) of tomato plants.



752 **Fig.5.** (A) Microbial respiration, (B) Total nitrogen mineralization over time (from 0 to 91
753 days), and (C) Ammonia volatilization for the four conditions: soil, soil with biochar
754 application at 25 tons/ha (soil + B25), soil with liquid digestate (soil + LD), and soil with
755 liquid digestate and biochar application at 25 tons/ha (soil + LD + B25).

756 **References**

- 757 1. Abdeljaoued, E., Brulé, M., Tayibi, S., Manolagos, D., Oukarroum, A., Monlau, F.,
758 Barakat, A., 2020. Bibliometric analysis of the evolution of biochar research trends and
759 scientific production, *Clean Technologies and Environmental Policy*. Springer Berlin
760 Heidelberg. <https://doi.org/10.1007/s10098-020-01969-x>
- 761 2. AFNOR FD U44-163, 2018. Organic amendments and growing media - Characterization of
762 organic matter by the potential mineralization of carbon and nitrogen.
- 763 3. Akhiar, A., Battimelli, A., Torrijos, M., Carrere, H., 2017. Comprehensive characterization
764 of the liquid fraction of digestates from full-scale anaerobic co-digestion. *Waste Manag.*
765 59, 118–128. <https://doi.org/10.1016/j.wasman.2016.11.005>
- 766 4. Alagöz, B.A., Yenigün, O., 2015. Enhancement of anaerobic digestion efficiency of
767 wastewater sludge and olive waste: Synergistic effect of co-digestion and ultrasonic /
768 microwave sludge pre-treatment. *Waste Manag.* 46, 182–188.
769 <https://doi.org/10.1016/j.wasman.2015.08.020>
- 770 5. Alhamed, H., Biad, M., Saad, S., Masaki, M., 2018. Business Opportunities Report for
771 Reuse of Wastewater in Morocco.
- 772 6. Ameloot, N., Sleutel, S., Das, K.C., KANAGARATNAM, J., NEVE, S. DE, 2015. Biochar
773 amendment to soils with contrasting organic matter level: effects on N mineralization
774 and biological soil properties. *GCB Bioenergy* 135–144.
775 <https://doi.org/10.1111/gcbb.12119>
- 776 7. APHA, 2005. Standard methods for the examination of water and wastewater. Am. Public
777 Heal. Assoc. 21st ed., 1220 p.
- 778 8. Barakat, A., Monlau, F., Solhy, A., Carrere, H., 2015. Mechanical dissociation and
779 fragmentation of lignocellulosic biomass: Effect of initial moisture, biochemical and
780 structural proprieties on energy requirement. *Appl. Energy* 142, 240–246.
781 <https://doi.org/10.1016/j.apenergy.2014.12.076>
- 782 9. Belloulid, M.O., Hamdi, H., Mandi, L., Ouazzani, N., 2017. Solar drying of wastewater
783 sludge: a case study in Marrakesh, Morocco. *Environ. Technol. (United Kingdom)* 40,
784 1316–1322. <https://doi.org/10.1080/09593330.2017.1421713>
- 785 10. Bruun, S., EL-Zehery, T., 2012. Biochar effect on the mineralization of soil organic
786 matter. *Pesqui. Agropecuária Bras.* 47, 665–671. <https://doi.org/10.1590/S0100-204X2012000500005>
- 788 11. Bu, X., Xue, J., Wu, Y., Ma, W., 2020. Effect of Biochar on Seed Germination and
789 Seedling Growth of *Robinia pseudoacacia* L. In *Karst Calcareous Soils*. *Commun. Soil*
790 *Sci. Plant Anal.* 51, 352–363. <https://doi.org/10.1080/00103624.2019.1709484>
- 791 12. Calamai, A., Palchetti, E., Masoni, A., Marini, L., Chiaramonti, D., Dibari, C., Brilli, L.,
792 2019. The Influence of Biochar and Solid Digestate on Rose-Scented Geranium
793 (*Pelargonium graveolens* L'Hér.) Productivity and Essential Oil Quality. *Agronomy* 9,
794 260. <https://doi.org/10.3390/agronomy9050260>
- 795 13. Cazaudehore, G., Schraauwers, B., Peyrelasse, C., Lagnet, C., Monlau, F., 2019.
796 Determination of chemical oxygen demand of agricultural wastes by combining acid
797 hydrolysis and commercial COD kit analysis. *J. Environ. Manage.* 250, 109464.
798 <https://doi.org/10.1016/j.jenvman.2019.109464>

- 799 14. Chandra, R., Takeuchi, H., Hasegawa, T., 2012. Methane production from lignocellulosic
800 agricultural crop wastes : A review in context to second generation of biofuel production.
801 *Renew. Sustain. Energy Rev.* 16, 1462–1476. <https://doi.org/10.1016/j.rser.2011.11.035>
- 802 15. Clough, T., Condrón, L., Kammann, C., Müller, C., 2013. A Review of Biochar and Soil
803 Nitrogen Dynamics. *Agronomy* 3, 275–293. <https://doi.org/10.3390/agronomy3020275>
- 804 16. Demichelis, F., Laghezza, M., Chiappero, M., Fiore, S., 2020. Technical , economic and
805 environmental assesement of bioethanol biorefinery from waste biomass. *J. Clean. Prod.*
806 277, 124111. <https://doi.org/10.1016/j.jclepro.2020.124111>
- 807 17. Elalami, D., Carrere, H., Monlau, F., Abdelouahdi, K., Oukarroum, A., Barakat, A., 2019.
808 Pretreatment and co-digestion of wastewater sludge for biogas production: Recent
809 research advances and trends. *Renew. Sustain. Energy Rev.* 114, 109287.
810 <https://doi.org/10.1016/j.rser.2019.109287>
- 811 18. Elalami, D., Monlau, F., Carrere, H., Abdelouahdi, K., Oukarroum, A., Zeroual, Y.,
812 Barakat, A., 2020. Effect of coupling alkaline pretreatment and sewage sludge co-
813 digestion on methane production and fertilizer potential of digestate. *Sci. Total Environ.*
814 743, 140670. <https://doi.org/10.1016/j.scitotenv.2020.140670>
- 815 19. Elbeshbishy, E., Nakhla, G., Hafez, H., 2012. Biochemical methane potential (BMP) of
816 food waste and primary sludge: Influence of inoculum pre-incubation and inoculum
817 source. *Bioresour. Technol.* 110, 18–25. <https://doi.org/10.1016/j.biortech.2012.01.025>
- 818 20. Fabbri, D., Torri, C., 2016. Linking pyrolysis and anaerobic digestion (Py-AD) for the
819 conversion of lignocellulosic biomass. *Curr. Opin. Biotechnol.* 38, 167–173.
820 <https://doi.org/10.1016/j.copbio.2016.02.004>
- 821 21. Fernández, J.M., Nieto, M.A., López-de-Sá, E.G., Gascó, G., Méndez, A., Plaza, C., 2014.
822 Carbon dioxide emissions from semi-arid soils amended with biochar alone or combined
823 with mineral and organic fertilizers. *Sci. Total Environ.* 482–483, 1–7.
824 <https://doi.org/10.1016/j.scitotenv.2014.02.103>
- 825 22. Fidel, R.B., Laird, D.A., Parkin, T.B., 2019. Effect of Biochar on Soil Greenhouse Gas
826 Emissions at the Laboratory and Effect of Biochar on Soil Greenhouse Gas Emissions at
827 the Laboratory and Field Scales. *Soil Syst.* <https://doi.org/10.3390/soilsystems3010008>
- 828 23. Ghysels, S., Acosta, N., Estrada, A., Pala, M., Vrieze, J. De, Ronsse, F., Rabaey, K., 2020.
829 Integrating anaerobic digestion and slow pyrolysis improves the product portfolio of a
830 cocoa waste biorefinery. *Sustain. Energy Fuels* 4, 3712–3725.
831 <https://doi.org/10.1039/d0se00689k>
- 832 24. Giuliano, A., Bolzonella, D., Pavan, P., Cavinato, C., Cecchi, F., 2013. Co-digestion of
833 livestock effluents, energy crops and agro-waste: Feeding and process optimization in
834 mesophilic and thermophilic conditions. *Bioresour. Technol.* 128, 612–618.
835 <https://doi.org/10.1016/j.biortech.2012.11.002>
- 836 25. Glaser, B., Wiedner, K., Seelig, S., Schmidt, H.P., Gerber, H., 2015. Biochar organic
837 fertilizers from natural resources as substitute for mineral fertilizers. *Agron. Sustain.*
838 *Dev.* 35, 667–678. <https://doi.org/10.1007/s13593-014-0251-4>
- 839 26. González-Arias, J., Fernández, C., Rosas, J.G., Bernal, M.P., Clemente, R., Sánchez,
840 M.E., Gómez, X., 2019. Integrating Anaerobic Digestion of Pig Slurry and Thermal
841 Valorisation of Biomass. *Waste and Biomass Valorization* 11, 6125–6137.

- 842 <https://doi.org/10.1007/s12649-019-00873-w>
- 843 27. González, R., González, J., Rosas, J.G., Smith, R., Gómez, X., 2020. Biochar and Energy
844 Production : Valorizing Swine Manure through Coupling Co-Digestion and Pyrolysis. *J.*
845 *carbon Res.* 6,43. <https://doi.org/10.3390/c6020043>
- 846 28. Greenberg, I., Kaiser, M., Gunina, A., Ledesma, P., Polifka, S., Wiedner, K., Mueller,
847 C.W., Glaser, B., Ludwig, B., 2019. Substitution of mineral fertilizers with biogas
848 digestate plus biochar increases physically stabilized soil carbon but not crop biomass in
849 a field trial. *Sci. Total Environ.* 680, 181–189.
850 <https://doi.org/10.1016/j.scitotenv.2019.05.051>
- 851 29. Hafner, S.D., Fruteau de Laclos, H., Koch, K., Holliger, C., 2020. Improving Inter-
852 Laboratory Reproducibility in Measurement of Biochemical Methane Potential (BMP).
853 *Water* 12, 1752. <https://doi.org/10.3390/w12061752>
- 854 30. Hood-Nowotny, R., Umana, N.H.-N., Inselbacher, E., Oswald- Lachouani, P., Wanek, W.,
855 2010. Alternative Methods for Measuring Inorganic, Organic, and Total Dissolved
856 Nitrogen in Soil. *Soil Sci. Soc. Am. J.* 74, 1018–1027.
857 <https://doi.org/10.2136/sssaj2009.0389>
- 858 31. Hossain, A.K., Serrano, C., Brammer, J.B., Omran, A., Ahmed, F., Smith, D.I., Davies,
859 P.A., 2016. Combustion of fuel blends containing digestate pyrolysis oil in a multi-
860 cylinder compression ignition engine. *Fuel* 171, 18–28.
861 <https://doi.org/10.1016/j.fuel.2015.12.012>
- 862 32. Im, S., Petersen, S.O., Lee, D., Kim, D.H., 2020. Effects of storage temperature on CH₄
863 emissions from cattle manure and subsequent biogas production potential. *Waste Manag.*
864 101, 35–43. <https://doi.org/10.1016/j.wasman.2019.09.036>
- 865 33. Jęczmionek, Ł., Porzycka-Semczuk, K., 2014. Hydrodeoxygenation, decarboxylation and
866 decarbonylation reactions while co-processing vegetable oils over a NiMo
867 hydrotreatment catalyst. Part I: Thermal effects - Theoretical considerations. *Fuel* 131,
868 1–5. <https://doi.org/10.1016/j.fuel.2014.04.055>
- 869 34. Jiang, Y., Mcadam, E., Zhang, Y., Heaven, S., Banks, C., Longhurst, P., 2019. Ammonia
870 inhibition and toxicity in anaerobic digestion : A critical review. *J. Water Process Eng.*
871 32, 100899. <https://doi.org/10.1016/j.jwpe.2019.100899>
- 872 35. Kim, Jinsu, Baek, G., Kim, Jaai, Lee, C., 2019. Energy production from different organic
873 wastes by anaerobic co-digestion: Maximizing methane yield versus maximizing
874 synergistic effect. *Renew. Energy* 136, 683–690.
875 <https://doi.org/10.1016/j.renene.2019.01.046>
- 876 36. Kjeldahl, J., 1883. A New Method for the Determination of Nitrogen in Organic Matter.
877 *Zeitschrift für Anal. Chemie* 22, 366–382.
- 878 37. Li, X., Xu, X., Huang, S., Zhou, Y., Jia, H., 2017. An efficient method to improve the
879 production of methane from anaerobic digestion of waste activated sludge. *Water Sci.*
880 *Technol.* 76,8, 2075–2084. <https://doi.org/10.2166/wst.2017.313>
- 881 38. Liu, C., Huang, J., Huang, X., Li, H., Zhang, Z., 2011. Theoretical studies on formation
882 mechanisms of CO and CO₂ in cellulose pyrolysis. *Comput. Theor. Chem.* 964, 207–212.
883 <https://doi.org/10.1016/j.comptc.2010.12.027>
- 884 39. Lv, P.M., Xiong, Z.H., Chang, J., Wu, C.Z., Chen, Y., Zhu, J.X., 2004. An experimental

- 885 study on biomass air – steam gasification in a fluidized bed 95, 95–101.
886 <https://doi.org/10.1016/j.biortech.2004.02.003>
- 887 40. Mandal, S., Pu, S., Adhikari, S., Ma, H., Kim, D., 2020. Technology Progress and future
888 prospects in biochar composites: Application and reflection in the soil environment.
889 *Crit. Rev. Environ. Sci. Technol.* 0, 1–53.
890 <https://doi.org/10.1080/10643389.2020.1713030>
- 891 41. Monlau, F., Barakat, A., Trably, E., Dumas, C., Steyer, J.P., Carrère, H., 2013.
892 Lignocellulosic materials into biohydrogen and biomethane: Impact of structural features
893 and pretreatment. *Crit. Rev. Environ. Sci. Technol.* 43, 260–322.
894 <https://doi.org/10.1080/10643389.2011.604258>
- 895 42. Monlau, F., Francavilla, M., Sambusiti, C., Antoniou, N., Solhy, A., Libutti, A.,
896 Zabaniotou, A., Barakat, A., Monteleone, M., 2016. Toward a functional integration of
897 anaerobic digestion and pyrolysis for a sustainable resource management. Comparison
898 between solid-digestate and its derived pyrochar as soil amendment. *Appl. Energy* 169,
899 652–662. <https://doi.org/10.1016/j.apenergy.2016.02.084>
- 900 43. Monlau, F., Kaparaju, P., Trably, E., Steyer, J.P., Carrere, H., 2015a. Alkaline
901 pretreatment to enhance one-stage CH₄ and two-stage H₂/CH₄ production from
902 sunflower stalks: Mass, energy and economical balances. *Chem. Eng. J.* 260, 377–385.
903 <https://doi.org/10.1016/j.cej.2014.08.108>
- 904 44. Monlau, F., Sambusiti, C., Antoniou, N., Barakat, A., Zabaniotou, A., 2015b. A new
905 concept for enhancing energy recovery from agricultural residues by coupling anaerobic
906 digestion and pyrolysis process. *Appl. Energy* 148, 32–38.
907 <https://doi.org/10.1016/j.apenergy.2015.03.024>
- 908 45. Monlau, F., Sambusiti, C., Barakat, A., Guo, X.M., Latrille, E., Trably, E., Steyer, J.P.,
909 Carrere, H., 2012. Predictive models of biohydrogen and biomethane production based
910 on the compositional and structural features of lignocellulosic materials. *Environ. Sci.*
911 *Technol.* 46, 12217–12225. <https://doi.org/10.1021/es303132t>
- 912 46. Monlau, F., Sambusiti, C., Ficara, E., Aboulkas, A., Barakat, A., Carrère, H., 2015c. New
913 opportunities for agricultural digestate valorization: Current situation and perspectives.
914 *Energy Environ. Sci.* 8, 2600–2621. <https://doi.org/10.1039/c5ee01633a>
- 915 47. Morales-polo, C., Cledera-Castro, M. del M., Soria, Y.M., 2018. applied sciences
916 Reviewing the Anaerobic Digestion of Food Waste: From Waste Generation and
917 Anaerobic Process to Its Perspectives. *Appl. Sci.* 8. <https://doi.org/10.3390/app8101804>
- 918 48. Morozova, I., Nikulina, N., Oechsner, H., Krümpel, J., Lemmer, A., 2020. Effects of
919 Increasing Nitrogen Content on Process Stability and Reactor Performance in Anaerobic
920 Digestion. *energies* 13. <https://doi.org/10.3390/en13051139>
- 921 49. Neumann, J., Binder, S., Apfelbacher, A., Gasson, J.R., Ramírez García, P., Hornung, A.,
922 2015. Production and characterization of a new quality pyrolysis oil, char and syngas
923 from digestate - Introducing the thermo-catalytic reforming process. *J. Anal. Appl.*
924 *Pyrolysis* 113, 137–142. <https://doi.org/10.1016/j.jaap.2014.11.022>
- 925 50. NF U 42-125, 1985. Fertilizers - Determination of ammoniacal nitrogen in the presence of
926 other substances releasing ammonia under the effect of sodium hydroxide - Titrimetric
927 method.

- 928 51. Nkoa, R., 2014. Agricultural benefits and environmental risks of soil fertilization with
929 anaerobic digestates: A review. *Agron. Sustain. Dev.* [https://doi.org/10.1007/s13593-](https://doi.org/10.1007/s13593-013-0196-z)
930 013-0196-z
- 931 52. Opatokun, S.A., Strezov, V., Kan, T., 2015. Product based evaluation of pyrolysis of food
932 waste and its digestate. *Energy* 92, 349–354.
933 <https://doi.org/10.1016/j.energy.2015.02.098>
- 934 53. Opatokun, S.A., Yousef, L.F., Strezov, V., 2017. Agronomic assessment of pyrolysed
935 food waste digestate for sandy soil management. *J. Environ. Manage.* 187, 24–30.
936 <https://doi.org/10.1016/j.jenvman.2016.11.030>
- 937 54. Pecchi, M., Baratieri, M., 2019. Coupling anaerobic digestion with gasification, pyrolysis
938 or hydrothermal carbonization: A review. *Renew. Sustain. Energy Rev.* 105, 462–475.
939 <https://doi.org/10.1016/j.rser.2019.02.003>
- 940 55. Plaimart, J., Acharya, K., Mroziak, W., Davenport, R.J., Vinitnantharat, S., Werner, D.,
941 2021. Coconut husk biochar amendment enhances nutrient retention by suppressing
942 nitrification in agricultural soil following anaerobic digestate application. *Environ.*
943 *Pollut.* 268, 115684. <https://doi.org/10.1016/j.envpol.2020.115684>
- 944 56. Pütün, A.E., Uzun, B.B., Apaydin, E., Pütün, E., 2005. Bio-oil from olive oil industry
945 wastes: Pyrolysis of olive residue under different conditions. *Fuel Process. Technol.* 87,
946 25–32. <https://doi.org/10.1016/j.fuproc.2005.04.003>
- 947 57. Rodier, J., 1975. Analysis of water, In: *Environmental chemical analysis*. Marr IL, Cresser
948 MS (Eds). Int. Textb. Company. Chapman Hall New York.
- 949 58. Ronga, D., Caradonia, F., Parisi, M., Bezzi, G., Parisi, B., Allesina, G., Pedrazzi, S.,
950 Francia, E., 2020. Using digestate and biochar as fertilizers to improve processing
951 tomato production sustainability. *Agronomy* 10.
952 <https://doi.org/10.3390/agronomy10010138>
- 953 59. Roubaud, A., Favrat, D., 2005. Improving performances of a lean burn cogeneration
954 biogas engine equipped with combustion prechambers. *Fuel* 84, 2001–2007.
955 <https://doi.org/10.1016/j.fuel.2004.02.023>
- 956 60. Sambusiti, C., Ficara, E., Malpei, F., Steyer, J.P., Carrère, H., 2013. Benefit of sodium
957 hydroxide pretreatment of ensiled sorghum forage on the anaerobic reactor stability and
958 methane production. *Bioresour. Technol.* 144, 149–155.
959 <https://doi.org/10.1016/j.biortech.2013.06.095>
- 960 61. Sawatdeenarunat, C., Nguyen, D., Surendra, K.C., Shrestha, S., Rajendran, K., Oechsner,
961 H., Xie, L., Kumar, S., Khanal, S.K., 2016. Anaerobic biorefinery: Current status,
962 challenges, and opportunities. *Bioresour. Technol.* 215, 304–313.
963 <https://doi.org/10.1016/j.biortech.2016.03.074>
- 964 62. Semida, W.M., Beheiry, H.R., Mamoudou, S., Simpson, C.R., El-Mageed, T.A.A., Rady,
965 M.M., Nelson, S.D., 2019. Biochar implications for sustainable agriculture and
966 environment: A review. *South African J. Bot.* 127.
967 <https://doi.org/10.1016/j.sajb.2019.11.015>
- 968 63. Seyedi, S., Venkiteshwaran, K., Zitomer, D., 2019. Toxicity of various pyrolysis liquids
969 from biosolids on methane production yield. *Front. Energy Res.* 7, 1–12.
970 <https://doi.org/10.3389/fenrg.2019.00005>

- 971 64. Sha, Z., Li, Q., Lv, T., Misselbrook, T., Liu, X., 2019. Response of ammonia
972 volatilization to biochar addition : A meta-analysis. *Sci. Total Environ.* 655, 1387–1396.
973 <https://doi.org/10.1016/j.scitotenv.2018.11.316>
- 974 65. Sluiter, A., Hames, B., Ruiz, R., Scarlata, C., Sluiter, J., Templeton, D., and Crocker, D.,
975 2008. Determination of Structural Carbohydrates and Lignin in Biomass: Laboratory
976 Analytical Procedure (LAP). Tech. Rep. NREL/ TP -510 -42618 1–15.
977 <https://doi.org/NREL/TP-510-42618>
- 978 66. Solé-Bundó, M., Cucina, M., Folch, M., Tàpias, J., Gigliotti, G., Garfí, M., Ferrer, I.,
979 2017. Assessing the agricultural reuse of the digestate from microalgae anaerobic
980 digestion and co-digestion with sewage sludge. *Sci. Total Environ.* 586, 1–9.
981 <https://doi.org/10.1016/j.scitotenv.2017.02.006>
- 982 67. Tayibi, S., Monlau, F., Mariase, F., Cazaudehore, G., Fayoud, N.-E., Oukarroum, A.,
983 Zeroual, Y., Barakat, A., 2021. Coupling anaerobic digestion and pyrolysis processes for
984 maximizing energy recovery and soil preservation according to the circular economy
985 concept. *J. Environ. Manage.* <https://doi.org/10.1016/j.jenvman.2020.111632>
- 986 68. Tayibi, S., Monlau, F., Oukarroum, A., Zeroual, Y., 2020. One - pot activation and
987 pyrolysis of Moroccan *Gelidium sesquipedale* red macroalgae residue : production of an
988 efficient adsorbent biochar. *Biochar.* <https://doi.org/10.1007/s42773-019-00033-2>
- 989 69. Torri, C., Fabbri, D., 2014. Biochar enables anaerobic digestion of aqueous phase from
990 intermediate pyrolysis of biomass. *Bioresour. Technol.* 172, 335–341.
991 <https://doi.org/10.1016/j.biortech.2014.09.021>
- 992 70. Tripathi, M., Sahu, J.N., Ganesan, P., 2016. Effect of process parameters on production of
993 biochar from biomass waste through pyrolysis: A review. *Renew. Sustain. Energy Rev.*
994 55, 467–481. <https://doi.org/10.1016/j.rser.2015.10.122>
- 995 71. Troy, S.M., Nolan, T., Leahy, J.J., Lawlor, P.G., Healy, M.G., Kwapinski, W., 2013.
996 Effect of sawdust addition and composting of feedstock on renewable energy and
997 biochar production from pyrolysis of anaerobically digested pig manure. *Biomass and*
998 *Bioenergy* 49, 1–9. <https://doi.org/10.1016/j.biombioe.2012.12.014>
- 999 72. Van, D.P., Fujiwara, T., Tho, B.L., Toan, P.P.S., Minh, G.H., 2020. A review of anaerobic
1000 digestion systems for biodegradable waste : Configurations , operating parameters , and
1001 current trends. *Environ. Eng. Res.* 25, 1–17.
- 1002 73. Wei, Y., Hong, J., Ji, W., 2018. Thermal characterization and pyrolysis of digestate for
1003 phenol production. *Fuel* 232, 141–146. <https://doi.org/10.1016/j.fuel.2018.05.134>
- 1004 74. Wei, Z., Li, Y., Hou, Y., 2018. Quick estimation for pollution load contributions of
1005 aromatic organics in wastewater from pulp and paper industry. *Nord. Pulp Pap. Res. J.*
1006 33, 568–572.
- 1007 75. Yenigün, O., Demirel, B., 2013. Ammonia inhibition in anaerobic digestion : A review.
1008 *Process Biochem.* 48, 901–911. <https://doi.org/10.1016/j.procbio.2013.04.012>
- 1009 76. Yoo, G., Kang, H., 2012. Effects of Biochar Addition on Greenhouse Gas Emissions and
1010 Microbial Responses in a Short-Term Laboratory Experiment. *J. Environ. Qual.* 41,
1011 1193–1202. <https://doi.org/10.2134/jeq2011.0157>
- 1012 77. Zhao, Z., Li, Y., Quan, X., Zhang, Y., 2018. Improving the co-digestion performance of
1013 waste activated sludge and wheat straw through ratio optimization and ferrous oxide

1014 supplementation. Bioresour. Technol. 267, 591–598.
1015 <https://doi.org/10.1016/j.biortech.2018.07.052>
1016